ACADEMIC PRESS

Available online at www.sciencedirect.com

SCIENCE DIRECT®

DEVELOPMENTAL BIOLOGY

Developmental Biology 255 (2003) 77–98

www.elsevier.com/locate/ydbio

Neurovascular congruence results from a shared patterning mechanism that utilizes Semaphorin3A and Neuropilin-1

Damien Bates,[a,b,*] G. Ian Taylor,[b] Joe Minichiello,[a] Peter Farlie,[a] Adam Cichowitz,[a,b] Nadine Watson,[c] Michael Klagsbrun,[d] Roni Mamluk,[e] and Donald F. Newgreen[a]

[a] *Embryology Lab, MCR1, Royal Children's Hospital, Flemington Rd, Parkville, VIC, 3052, Australia*
[b] *Plastic & Reconstructive Surgery Research Unit, Royal Melbourne Hospital, 766 Elizabeth St. Melbourne, VIC, 3000, Australia*
[c] *Department of Anatomy and Cell Biology, University of Melbourne, Melbourne, VIC, 3010, Australia*
[d] *Departments of Surgery and Pathology, Children's Hospital and Harvard Medical School, 300 Longwood Avenue, Boston, MA 02115, USA*
[e] *Departments of Surgery, Children's Hospital and Harvard Medical School, 300 Longwood Avenue, Boston, MA 02115, USA*

Received for publication 5 July 2002, revised 4 November 2002, accepted 4 November 2002

Abstract

Peripheral nerves and blood vessels have similar patterns in quail forelimb development. Usually, nerves extend adjacent to existing blood vessels, but in a few cases, vessels follow nerves. Nerves have been proposed to follow vascular smooth muscle, endothelium, or their basal laminae. Focusing on the major axial blood vessels and nerves, we found that when nerves grow into forelimbs at E3.5–E5, vascular smooth muscle was not detectable by smooth muscle actin immunoreactivity. Additionally, transmission electron microscopy at E5.5 confirmed that early blood vessels lacked smooth muscle and showed that the endothelial cell layer lacks a basal lamina, and we did not observe physical contact between peripheral nerves and these endothelial cells. To test more generally whether lack of nerves affected blood vessel patterns, forelimb-level neural tube ablations were performed at E2 to produce aneural limbs; these had completely normal vascular patterns up to at least E10. To test more generally whether vascular perturbation affected nerve patterns, $VEGF_{165}$, $VEGF_{121}$, Ang-1, and soluble Flt-1/Fc proteins singly and in combination were focally introduced via beads implanted into E4.5 forelimbs. These produced significant alterations to the vascular patterns, which included the formation of neo-vessels and the creation of ectopic avascular spaces at E6, but in both under- and overvascularized forelimbs, the peripheral nerve pattern was normal. The spatial distribution of semaphorin3A protein immunoreactivity was consistent with a negative regulation of neural and/or vascular patterning. Semaphorin3A bead implantations into E4.5 forelimbs caused failure of nerves and blood vessels to form and to deviate away from the bead. Conversely, semaphorin3A antibody bead implantation was associated with a local increase in capillary formation. Furthermore, neural tube electroporation at E2 with a construct for the soluble form of neuropilin-1 caused vascular malformations and hemorrhage as well as altered nerve trajectories and peripheral nerve defasciculation at E5–E6. These results suggest that neurovascular congruency does not arise from interdependence between peripheral nerves and blood vessels, but supports the hypothesis that it arises by a shared patterning mechanism that utilizes semaphorin3A.

Keywords: Neurovascular; Pattern formation; Nerves; Blood vessels; Endothelium; Smooth muscle; Forelimb; Semaphorin3A; VEGF; Flt-1; Neuropilin-1; Quail

Introduction

The congruence of peripheral nerve and blood vessel anatomical patterns has been well described in human and other vertebrate adults (Feig and Guillery, 2000; Lewis, 1902; Lucas and Stettenheim, 1972; Miller, 1939; Taylor et al., 1994), giving rise to the term "neurovascular bundle" (Wheater et al., 1985). In particular, the adult vertebrate forelimb demonstrates a highly stereotypic and close spatial relationship between peripheral nerves and blood vessels (Sunderland, 1945; Taylor et al., 1994). Neurovascular congruency in the vertebrate forelimb is established during embryogenesis (Bates et al., 2002); however, the means by

* Corresponding author. Embryology Lab, MCRI, Royal Children's Hospital, Flemington Rd, Parkville, VIC, 3052, Australia. Fax: +613-93481391.
E-mail address: bates_damien@hotmail.com (D. Bates).

0012-1606/03/$ – see front matter © 2003 Elsevier Science (USA). All rights reserved.
doi:10.1016/S0012-1606(02)00045-3

which such congruency arises remains poorly characterized (Martin and Lewis, 1989; Mukouyama et al., 2002).

Lumenized blood vessels in the embryonic avian forelimb are formed via vasculogenesis and angiogenesis (Brand-Saberi et al., 1995) and form discrete patterns prior to peripheral nerve in-growth. However, there are several examples where nerves precede the in-growth and foreshadow the trajectory of their corresponding vessels (Bates et al., 2002). Nerves are invariably found to lie on one of four capillary layers in the dorsoventral (D-V) axis and are commonly juxtaposed in the anteroposterior (A-P) and proximodistal (P-D) axes of the forelimb (Bates et al., 2002). Neurovascular congruency in all spatial axes is highest toward the geometric center of the forelimb. Hence, major named mixed (e.g., motor and sensory) nerves (e.g., median nerve) are frequently colocalized with major named arteries (e.g., median artery) in the A-P and P-D axes, whereas cutaneous nerves and vessels are often only colocalized in the D-V axis (Martin and Lewis, 1989). These major neurovascular bundles typically supply muscles and bones in contradistinction to their minor branches that supply the skin.

The first theory of how neurovascular congruency is established suggests that peripheral nerves and blood vessels pattern on one another. Tello (1917) proposed the initial version of this theory, suggesting that the vasculature acts as a template for nerve distribution, and this has since been supported by others (Gu et al., 1995; Hobson et al., 1997; Lengele and Dhem, 1989; Miller, 1939; Singer, 1933a,b; Weddell, 1942). Recent evidence suggests that blood vessels may provide guidance cues for peripheral nerves by expressing molecules, such as fibronectin (Spence and Poole, 1994), artemin (Enomoto et al., 2001; Honma et al., 2002), and β-netrin (Koch et al., 2000). Vascular smooth muscle may play an important role in this regard; however, spatiotemporal studies of vascular smooth muscle distribution in the forelimb of vertebrate embryos (Takahashi et al., 1996) have not been correlated with peripheral nerve distribution, and it is still not known whether vascular smooth muscle is present in those blood vessels along which peripheral nerves initially extend.

Conversely, it has also been suggested that nerves may have a role in modifying the vascular pattern (Martin and Lewis, 1989; Mukouyama et al., 2002). Trophic factors, such as vascular endothelial growth factor (VEGF) released by neurons and peripheral nerves, stimulate endothelial cell proliferation, migration (Ogunshola et al., 2000), and differentiation (Mukouyama et al., 2002). Selective denervation leads to a decrease in capillary density in adult skeletal muscle (Borisov et al., 2000), but denervation of embryonic forelimbs does not significantly alter the pattern of cutaneous blood vessels (Martin and Lewis, 1989). It is not known at present what effect denervation has on vessels other than skin capillaries and whether specific vascular remodeling events are affected. Similarly, no studies have examined the effect of an abnormal vascular pattern (in an otherwise normal limb) on the developing peripheral nerve pattern.

The second theory of how neurovascular congruency arises is through shared patterning mechanisms (Roush, 1998; Shima and Mailhos, 2000). Candidate molecules include the secreted molecules vascular endothelial growth factor (VEGF), semaphorin3A (Sema3A), and the cell surface receptor neuropilin-1 (NRP1). $VEGF_{165}$ and Sema3A compete for binding to the transmembrane NRP1 receptor, which is present on both nerves and endothelium (Herzog et al., 2001; Kitsukawa et al., 1995; Soker et al., 1998). The effect of $VEGF_{165}$ on both peripheral nerves and blood vessels opposes the effect of Sema3A on these tissues in vitro (Bagnard et al., 2001; Miao et al., 1999). VEGF is a potent endothelial cell motility and survival factor (Drake et al., 2000; Gupta et al., 1999; Morales-Ruiz et al., 2000) and has also been shown to increase axonal outgrowth and neuronal survival (Jin et al., 2000; Oosthuyse et al., 2001; Schratzberger et al., 2000; Sondell et al., 1999a,b, 2000). In contrast, Sema3A has been shown to inhibit endothelial cell motility (Miao et al., 1999) and survival (Bagnard et al., 2001). Similarly, Sema3A has been shown to inhibit axonal outgrowth (Fan and Raper, 1995; Luo et al., 1993; Messersmith et al., 1995; Puschel et al., 1995) and to decrease survival of sensory neurons in vitro (Gagliardini and Fankhauser, 1999). The NRP1 receptor is required for vascular patterning events, such as vasculogenesis and angiogenesis (Soker, 2001; Soker et al., 1998; Whitaker et al., 2001; Yamada et al., 2001), and is also required for axonal patterning (Bagnard et al., 2001; Fujisawa et al., 1997; Kawakami et al., 1996; Rohm et al., 2000). Furthermore, knockout and overexpression studies involving the NRP1/Sema3A system (Behar et al., 1996; Kawasaki et al., 1999; Kitsukawa et al., 1995, 1997; Mukouyama et al., 2002; Takashima et al., 2002; Taniguchi et al., 1997) have demonstrated abnormalities in both peripheral nerve and vascular patterning. However, there have been no in vivo Sema3A overexpression studies that have examined the effect on the developing vasculature, and despite the ability of the soluble form of NRP1 (sNRP1) to bind both $VEGF_{165}$ and Sema3A (Gagnon et al., 2000), no in vivo misexpression studies of sNRP1 have been reported to date. Recent in vitro studies have suggested that sNRP1 can either enhance or inhibit vascular development, depending on whether sNRP1 exists in a monomeric or dimeric form (Yamada et al., 2001); however, it is still not clear whether sNRP1 acts to increase or decrease $VEGF_{165}$ activity in vivo.

Both peripheral nerves and blood vessels have been observed to avoid similar regions of the developing forelimb (Bennett et al., 1980; Caplan and Koutroupas, 1973; Drushel et al., 1985; Feinberg et al., 1986; Hallmann et al., 1987; Martin et al., 1989; Martin and Lewis, 1989; Tosney and Landmesser, 1985; Wilson, 1986; Yin and Pacifici, 2001). These regions include the prechondrogenic mesenchyme, muscle-forming areas, and the subectodermal avascular zone. Sema3A mRNA expression studies in the fore-

limb of rat embryos (Giger et al., 1996; Wright et al., 1995) broadly match these prohibitive regions of the developing quail forelimb and are consistent with the hypothesis that Sema3A negatively regulates peripheral nerve and/or blood vessel outgrowth. However, no precise spatiotemporal correlation of Sema3A protein expression with forelimb neurovascular anatomy is currently available to support this hypothesis.

To determine whether neurovascular congruency arises as a result of nerve-vessel interdependence, vascular structures suggested as candidates for nerve guidance were sought immunologically and by transmission electron microscopy (TEM). Evidence for interdependence was also sought more generally; for this purpose, peripheral nerve and vascular patterns were altered separately but examined simultaneously. To determine whether neurovascular congruency arises in a different way, from shared molecular patterning mechanisms, we analyzed the expression pattern of a candidate neural and vascular pattern effector protein, Sema3A. Furthermore, we have conducted functional misexpression studies with both Sema3A and its soluble NRP1 receptor to clarify the means by which neurovascular pattern is determined and maintained in the forelimb.

Materials and methods

Embryos

Quail embryos (*Coturnix coturnix japonica*) were obtained from Lago Game (Melbourne, Australia) and incubated at 38°C to defined stages (Hamburger and Hamilton, 1951) between E2 (HH13) and E10 (HH36).

Ex ovo whole quail culture

To facilitate microsurgical operations and analysis, all quail embryos were cultured ex ovo in six-well plates (Medos, Melbourne, Australia). Quail egg contents were transferred to the six-well plates at 40 h incubation. Embryos and yolk sacs that were damaged were discarded. The plated embryos were then returned to the incubator. All embryos cultured in this way were found to have normal development and morphology to at least E15 (HH41) (unpublished observations).

Whole-mount peripheral nerve and blood vessel labeling

This technique has been previously described (Bates et al., 2002). The vasculature was labeled by intravascular perfusion with either India Ink (Pelikan No. 17 Black; Pol Equipment, Sydney, Australia) or TRITC-conjugated high m.w. dextran (D-7139; Molecular Probes, OR). Perfused embryos were immediately fixed in 4% PFA overnight at 4°C. Nerves were labeled with TUJI mouse monoclonal IgG antibody (Chemicon, Melbourne, Australia) diluted 1/250 overnight at 4°C followed by goat anti-mouse IgG Alexa 488 (Molecular Probes) secondary antibody diluted 1/100 overnight at 4°C. Antibodies were prepared in 1% BSA and 0.1% Triton X-100 (BDH Laboratory Supplies, UK). Forelimbs were analyzed in whole-mount or in thick sections with fluorescent stereomicroscopy (see Imaging methods below).

Frozen section immunolabeling

Our technique of frozen section immunolabeling has been previously described (Bates et al., 2002). Briefly, sections were pretreated for 10 min with 100 μl 1% BSA (Roche, Sydney, Australia) or 1% normal donkey serum (NDS; Jackson ImmunoResearch, PA) prior to application of the primary and secondary antibodies. Vascular smooth muscle cells were labeled with 1/200 mouse 1A4 monoclonal IgG anti-α smooth muscle actin (αSMA) antibody (A2547; Sigma, St. Louis, MO). Cartilage was labeled with 1/100 CS-56 mouse monoclonal IgM anti-chondroitin sulfate antibody (C8035; Sigma). Skeletal muscle was labeled with 1/50 MF20 mouse monoclonal IgG antibody (Developmental Studies Hybridoma Bank, Iowa City, IA). Peripheral nerves were labeled with 1/200 rabbit polyclonal anti-Neurofilament M (NF-M) C-terminal antibody (AB1987; Chemicon Int'l, Melbourne, Australia). Endothelial cells were labeled with 1/50 QH-1 mouse monoclonal IgG antibody (Developmental Studies Hybridoma Bank). Semaphorin3A (Sema3A) was labeled with 1/50 anti-Sema3A (N-15) goat polyclonal antibody (sc-1148; Selby Biolab, Melbourne, Australia). Antibodies were prepared in 1% BSA (or 1% NDS if labeling Sema3A) and 0.1% Triton X-100. Goat anti-mouse IgG Alexa 488 (1/400; Molecular Probes) was used to label smooth muscle, cartilage, and endothelial cells. $F(ab')_2$ donkey anti-rabbit IgG (1/200; H+L): Texas Red (Jackson ImmunoResearch, PA) was used to label peripheral nerves. Donkey anti-goat IgG (H+L):FITC (Jackson ImmunoResearch, PA) was used to label Sema3A.

Imaging methods

Our imaging methods have been described previously (Bates et al., 2002). Briefly, whole-mount forelimbs were transferred to a 3-cm petri dish in 90% glycerol for image analysis. Forelimbs were also cut freehand into thick (50–300 μm) sections by using a sapphire microscalpel (World Precision Instruments, Melbourne, Australia). Whole-mount and sectioned forelimbs were visualized with the Leica MZ FL III (Leica Microsystems, Switzerland) fluorescent stereomicroscope. Images were captured with a Leica DC200 digital camera III (Leica Microsystems) and processed with proprietary Leica IM1000 software (Ver 1.10 Release 17). Brightfield, GFP3, and Texas Red fluorescent filter images were obtained with the specimen in the same orientation and at the same magnification and digitally

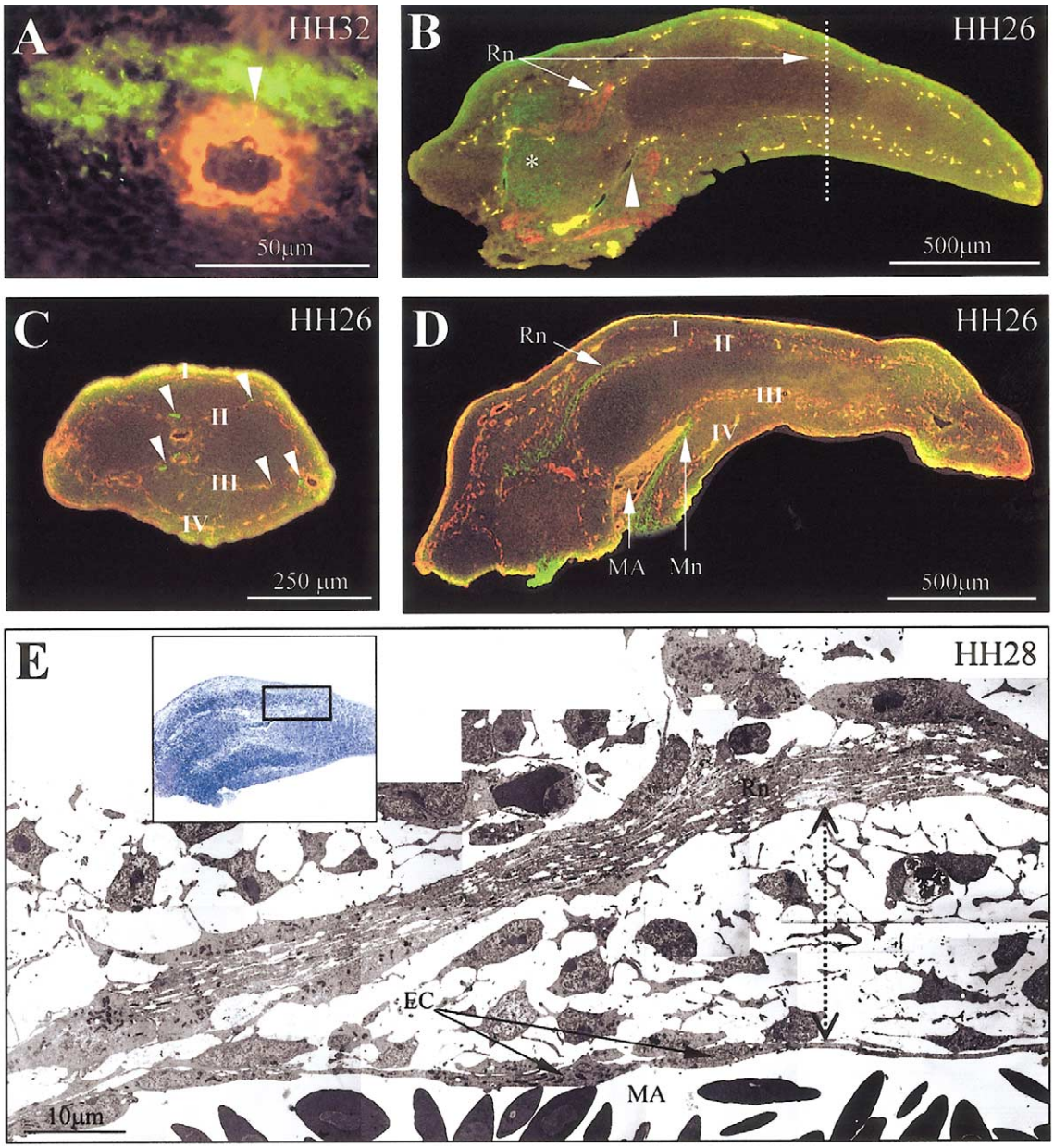

Fig. 1. In-growing forelimb nerves are spatially associated with blood vessels composed only of endothelium but do not physically contact the endothelial cells along which they track. (A) Coronal section showing that nerves (green) maintained a close spatial relationship (arrowhead) with vascular smooth muscle (red) surrounding blood vessels at E7 (HH32). (B) Sagittal forelimb section showing that vascular smooth muscle did not line the majority of blood vessels along which peripheral nerves track at the time of nerve in-growth at E5 (HH26). α Smooth muscle actin immunoreactivity (green) was confined to the proximal brachial artery (arrowhead) and dermomyotome (asterisk). Peripheral nerves [e.g., radial nerve (Rn)] were found greater than 500 μm distal (level of dotted line) to the most distal distribution of vascular smooth muscle (arrowhead). (C) Coronal section at the level of the median artery bifurcation at E5 showing the close spatial relationship between endothelial cells (red) immunolabeled with QH-1 and peripheral nerves (green) immunolabeled with neurofilament M. Nerves (arrowheads) were always associated with one of four discrete endothelial layers (numbered I–IV). (D) Sagittal section of an E5 forelimb showing nerves growing distally along preformed endothelial layers (I–IV). Nerves appeared to use these layers exclusively as scaffolds along which to track. MA, median artery; Mn, median nerve. (E) TEM sagittal section showing that, although the Rn tracked alongside its corresponding blood vessel (MA), it appeared to diverge from it as it progressed distally (to the right). It was located approximately 20 μm from the MA (distance indicated by dotted arrow). The largest blood vessel (i.e., MA) at E5.5 was composed of a single layer of endothelial cells (EC) that lacked a basal lamina. Inset indicates the region of the forelimb examined by TEM (black box).

overlaid. Images were captured as 1798 $\times$ 1438–pixel JPEG files. JPEG files were subsequently opened in Adobe Photoshop 5.0 (v5.0.2; Adobe Systems Inc., CA).

Forelimbs were positioned in a series of standard whole-mount positions to view the neurovascular anatomy. These views were dorsal and ventral side up. Standard sections

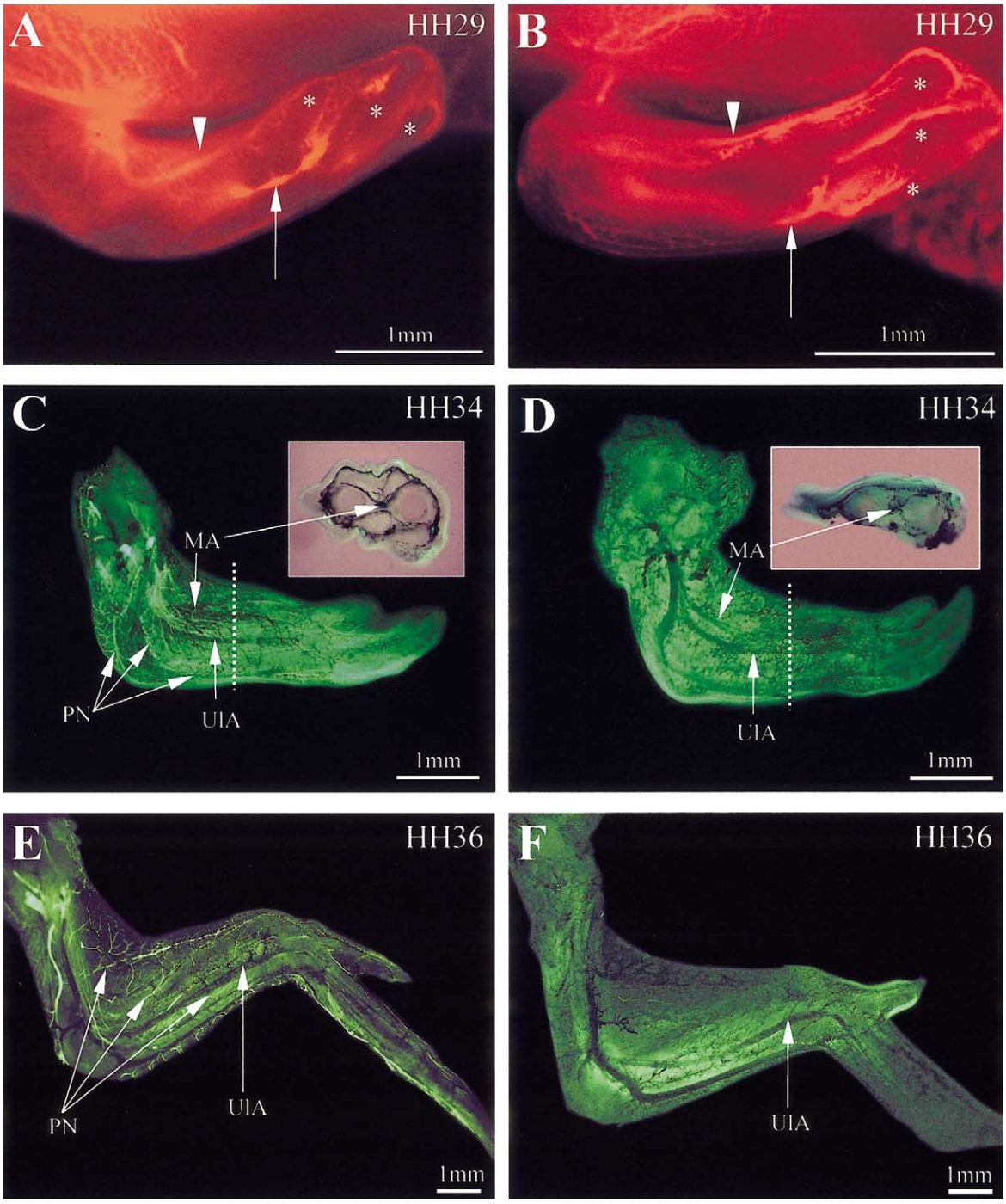

Fig. 2. The forelimb vascular pattern developed normally in the absence of nerves. Control forelimbs are located in the left-hand column (A, C, E), and aneural forelimbs are located in the right-hand column (B, D, F). Blood vessels were labeled with TRITC-conjugated high mw dextran (red) in (A) and (B). Both control (A) and aneural (B) E6 (HH29) forelimbs have the same vascular pattern: The main axial artery was located in the same position and was the same caliber (arrow); the anterior marginal vein (arrowhead) and the avascular spaces (asterisks) developed in the same positions and in the same sequence. Blood vessels were labeled with India Ink (black), and peripheral nerves were immunolabeled with TUJ1 (green) in (C–F). (C) E8 (HH34) control forelimb showing the presence of peripheral nerves (PN) and the ulnar (UIA) and median (MA) arteries. The dotted line illustrates the plane through which the coronal section was cut (insets in C and D), illustrating normal capillary layer formation in both control (C) and aneural (D) forelimbs. (E) E10 (HH36) control forelimb showing the differential remodeling of the ulnar artery (increase in caliber) that also occurred in the aneural (F) forelimb.

were coronal and sagittal unless otherwise specified. Coronal sections were oriented with the dorsal surface uppermost and the posterior (postaxial) border of the forelimb to the right. Sagittal sections were oriented with the dorsal surface uppermost and the distal border of the forelimb to the right.

Table 1
Neural tube excision results[a]

	Decreased peripheral nerves	Absent peripheral nerves	Normal blood vessels	Abnormal blood vessels	Total
E6 (HH29)	2	4	6	0	6
E8 (HH34)	5	7	12	0	12
E10 (HH36)	0	2	2	0	2
Total	7	13	20	0	20

[a] The numbers in this Table refer to the number of forelimbs.

Transmission electron microscopy

E5.5 (HH27–HH28) quail embryos were fixed overnight at 4°C in 2.5% glutaraldehyde and washed three times in PBS. Forelimbs were dissected from the embryo and manually sectioned in the sagittal plane 100 μm to the preaxial side of the median artery. The postaxial portion of the sectioned forelimb was placed in 30% ethanol and then washed in 5% sucrose in 0.1 M phosphate buffer. The tissue was dehydrated through a graded series of acetone solutions and embedded in epon–araldite. Ultra-thin sections were cut on a Reichert–Jung Ultra-S microtome and collected on Cu/Rh grids. The sections were stained with uranyl acetate and lead citrate and viewed on a Phillips CM-12 Transmission Electron Microscope at 80 kV.

Neural tube excision

Neural tube excisions were performed as previously described (Noakes et al., 1988; Teillet and Le Douarin, 1983). Briefly, neural tubes were excised from HH12–HH13 embryos (less than 19 somites) from somite 12 to presumptive somite 23. E6 (HH29) embryos were perfused with TRITC-conjugated high m.w. dextran, numbered, and photographed in whole mount prior to fixation. Whole-mount peripheral nerve immunolabeling was then performed on these specimens to determine which forelimbs had either no or a significant reduction in peripheral nerves. These results were then correlated with the images of the vascular pattern that had already been obtained. E8 and E10 embryos were perfused with India Ink, fixed, and immunolabeled. Peripheral nerve and blood vessel patterns were then imaged simultaneously in whole mount. For a forelimb to be assessable at each time point, each experimental embryo had to fulfill the following criteria: embryo survived to the appropriate stage without gross structural or functional abnormalities; adequate intravascular perfusion; and peripheral nerve immunolabeling.

Bead implantation

Forelimb bead implantations (Yang et al., 1997) were performed in E4.5–E5 (HH25–HH26) embryos. Dehydrated Cibacron blue 3GA beads (C1535; Sigma) were transferred to 2 μl of protein solution (see below) and allowed to soak for 1–2 h at 4°C. For hypervascularization experiments, $VEGF_{165}$ (10 μg/ml; generously supplied by Dr. Lynn Barnett, WEHI, Melbourne, Australia), $VEGF_{164}$ (10 μg/ml; generously supplied by Dr. Steven Stacker, Ludwig Institute, Melbourne, Australia), $VEGF_{165}$ (10 μg/ml; R&D Systems, MN), $VEGF_{121}$ (50 μg/ml; R&D Systems), and Angiopoietin-1 (1.24 mg/ml; generously supplied by Dr. George Yancopoulos, Regeneron Pharmaceuticals Inc., NY) were used. The two sources of $VEGF_{165}$ and $VEGF_{164}$ yielded the same experimental results and are treated together. When $VEGF_{165}$ and Angiopoietin-1 (Ang-1) were used in combination, their concentrations were 5 and 620 μg/ml, respectively. For hypovascularization experiments, recombinant soluble human Flt-1/F_c chimeric protein (0.5 mg/ml; R&D Systems) was used. Sema3A antibody (200 μg/ml) and chick Sema3A crude supernatant (see Cell culture below) were also used. All beads were implanted into right upper limbs. Left upper limbs served as internal controls. Embryos receiving beads soaked in PBS- and EGFP-transfected culture media served as additional controls. After

Table 2
Bead implantation results

	Total no. experiments	Total no. assessable	Total no. abnormal vessels	Abnormal vessels and normal nerves	Abnormal vessels and abnormal nerves	Normal vessels and normal nerves
Control[a]	136	52	0	0	0	52
$VEGF_{164/165}$	194	24	15	12	3	9
$VEGF_{165}$ + Ang-1	12	5	4	3	1	1
Ang-1	6	4	3	3	0	1
$VEGF_{121}$	8	5	3	3	0	2
sFlt-1/F_c	59	15[b]	7	7 (4)[c]	0	8
Sema3A[d]	30	12	6	0	6	6
Sema3A antibody	9	3	2	2	0	1

[a] Control beads were soaked in either PBS- or EGFP-transfected cell culture media.
[b] Beads that were implanted in normally avascular regions of the upper limb could not be assessed.
[c] Four of seven avascular regions were induced in the direct path of a nerve prior to nerve in-growth.
[d] Data for Sema3A bead implantations at E4.5 (HH25) and E5 (HH26) have been combined.

bead implantation, embryos were returned to the incubator and allowed to develop to E5.5–E6 (HH28–HH29), at which time forelimb analysis was performed. Changes in the neurovascular pattern in experimental embryos were compared with both sets of controls at E5.5–E6. Experimental analysis could only be performed in those embryos that fulfilled all of the following criteria: embryo survived to E5.5–E6 without gross abnormalities; bead remained in the limb; bead in correct location (both in terms of blood vessel and peripheral nerve trajectories); and adequate intravascular perfusion and peripheral nerve immunolabeling.

Neural tube explants

Neural tubes (between somites 15–20) were isolated from E2 quail embryos (HH13–HH14) and cultured on adsorbed fibronectin (20 μg/ml; Roche Diagnostics GmbH, Switzerland) as previously described (Newgreen and Minichiello, 1995). Neural tube cultures were divided into different groups receiving either control media (10% FCS/F12) or media supplemented with one of the following proteins: Sema3A (1:500 dilution of crude supernatant in 10% FCS/F12); Ang-1 (1.24 μg/ml 10% FCS/F12); soluble human Flt-1/F_c chimeric protein (500 ng/ml 10% FCS/F12); nerve growth factor 7S (100 ng/ml 10% FCS/F12; Roche, Sydney, Australia); $VEGF_{121}$ (50 ng/ml 10% FCS/F12); $VEGF_{165}$ (50 ng/ml 10% FCS/F12); and $VEGF_{165}$ and Ang-1 combination (50 ng/ml and 1.24 μg/ml 10% FCS/F12, respectively). Culture media were replaced daily for 3 days. Neural tubes were then fixed in 4%PFA for 10 min and then thoroughly washed in PBS. Cultures were pretreated for 10 min with 1% BSA prior to application of the antibodies. Peripheral nerves were labeled with 1/200 NF-M for 4 h at 4°C. Cultures were thoroughly washed in PBS and then labeled with 1/400 goat anti-rabbit IgG Alexa 488 (Molecular Probes) for 2 h. Cultures were washed in PBS again and visualized with the Leica MZ FL III fluorescent stereomicroscope. Axon outgrowth was analyzed with Scion Image Beta 4.0.2 software (Scion Corporation, MD). The following measurements were recorded: (1) axon density (total number of axons emerging from one side of the neural tube divided by neural tube length); (2) mean axon length (the lengths of the five longest axons were measured and the mean calculated). Data were recorded and analyzed in Microsoft Excel 97 by using the unpaired Student's *t* test.

Mouse sNRP1 cDNA cloning

Soluble NRP1 cDNA was cloned by 3′ RACE (rapid amplification of cDNA ends). First-strand oligo(dT)-primed cDNA was synthesized from 2 μg of mouse liver mRNA, and PCR was performed by using primers 5′NRP1b1 (GTGTTCATGAGGAAG) and 3′*Bam*HI dT (CCCTTCGGATCCTAACCTTTTTTTTTTTTTTTT); a secondary PCR was performed by using the first PCR as template and nested primers 5′NRP1b2 (ATCATGGATGACAGCAAGCGC) and *Bam*HI (CCCTTCGGATCCTAACC). A 580-bp PCR product was cloned by using the TOPO-TA cloning kit (Invitrogen). The 3′cDNA clone sequence was identified as a truncated NRP1 (sNRP1) cDNA. The full-length mouse sNRP1 was amplified from mouse liver cDNA by PCR using primers 5′-NRP1a (ATGGAGAGGGGGCTGCGGTT) and 3′sNRP1 (CAGATAAGTATGTGAGCCCAAGTGC) and subsequently cloned into pCDNA3.1 mammalian expression vector.

Plasmid preparation

Plasmid DNA was purified by using a plasmid purification kit (Qiagen, Melbourne, Australia) and was dissolved in MQ water. The expression plasmid pAG3 containing full-length chicken collapsin-1 (Sema3A) cDNA was the generous gift of Dr. Jonathan Raper (Department of Neuroscience, University of Pennsylvania).

Cell culture

BHK-21 cells were obtained from ICN Biomedicals (Sydney, Australia). Cells were cultured in 10% FCS/F12. BHK-21 cells were transiently lipofectamine-transfected to express Sema3A. Control cells were lipofectamine-transfected with pEGFP-N2 (Clontech, Palo Alto, CA). Cibacron beads were soaked in crude supernatants prior to implantation.

Neural tube electroporation

Neural tube electroporation was performed as previously described (Inoue and Krumlauf, 2001; Itasaki et al., 1999; Swartz et al., 2001). Briefly, a solution [9 μl purified pCDNA3.1 sNRP1 (1 mg/ml), 9 μl pEGFP-N2 (1 mg/ml) and 2 μl 0.4% Trypan Blue in PBS] was injected to fill the caudal neural tube of E2 (HH13) quail embryos. Control solutions contained 9 μl pEGFP-N2 (1 mg/ml) and 1 μl 0.4% Trypan Blue in PBS. A BTX ECM 830 square-wave electroporator with 3-mm L-shaped gold tip electrodes (Fisher Biotec, Melbourne, Australia) was used to generate electric pulses across the neural tube. Parameters for neural tube electroporation were: 25 V; 3 pulses; 50-ms pulse length. After electroporation, embryos were returned to the incubator for 24 h, after which they were examined for GFP expression. GFP expression was used as an indirect indicator of successful electroporation. Embryos were reincubated until E5–E6 (HH26–HH29), at which time forelimb analysis was performed.

Results

In-growing forelimb nerves are not directly associated with vascular smooth muscle or endothelial cells

Vascular smooth muscle has been suggested to provide guidance and/or trophic factors for nerves (see Introduc-

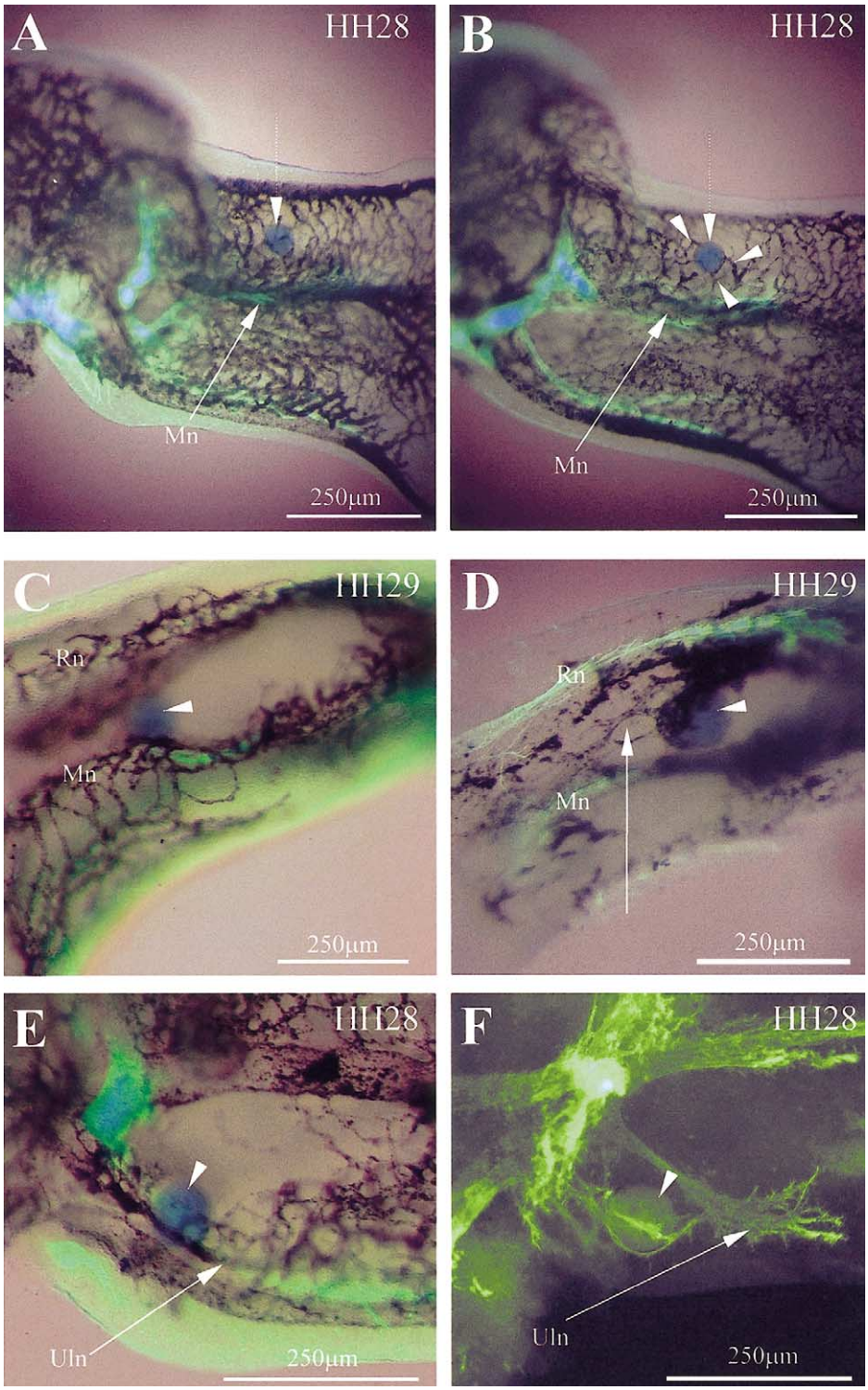

Fig. 3. Forelimb hypervascularization did not alter forelimb peripheral nerve pattern. (A) Ventral whole-mount of an E5.5 (HH28) control forelimb. Implantation of control (PBS- or EGFP-transfected culture media soaked) beads (dotted arrow) were not associated with changes in either the peripheral nerve [e.g., median nerve (Mn)] or vascular pattern. Capillaries remained ventral to and did not converge toward the bead. (B) Ventral whole-mount of an E5.5 forelimb into which a $VEGF_{165}$-soaked bead has been implanted (dotted arrow). Blood vessels (black) deviated toward the bead (indicated by multiple arrowheads), but the adjacent Mn maintained a normal trajectory. (C) Sagittal section of a control E6 (HH29) forelimb showing that the radial (Rn) and Mn neurovascular bundles diverged normally to enclose an avascular space. Nerves and blood vessels did not deviate toward the control (PBS) bead (arrowhead). (D) Sagittal section of an E6 forelimb into which a $VEGF_{165}$-soaked bead has been implanted (arrowhead). Ectopic blood vessels formed (arrow) and coalesced around the bead in the normally avascular space. The Rn and Mn did not use these neo-vessels as alternative pathways on which to track, nor did they appear to be guided toward them. (E) Ventral whole-mount view of a control E5.5 forelimb showing that the proximal trajectory of the ulnar nerve (Uln) was not altered by the presence of a control (PBS) bead (arrowhead). (F) Ventral whole-mount view of an E5.5 forelimb into which a $VEGF_{165}$-soaked bead has been implanted (arrowhead). The Uln pursued an abnormal trajectory around the bead that appeared to be acting as a physical barrier to axon outgrowth.

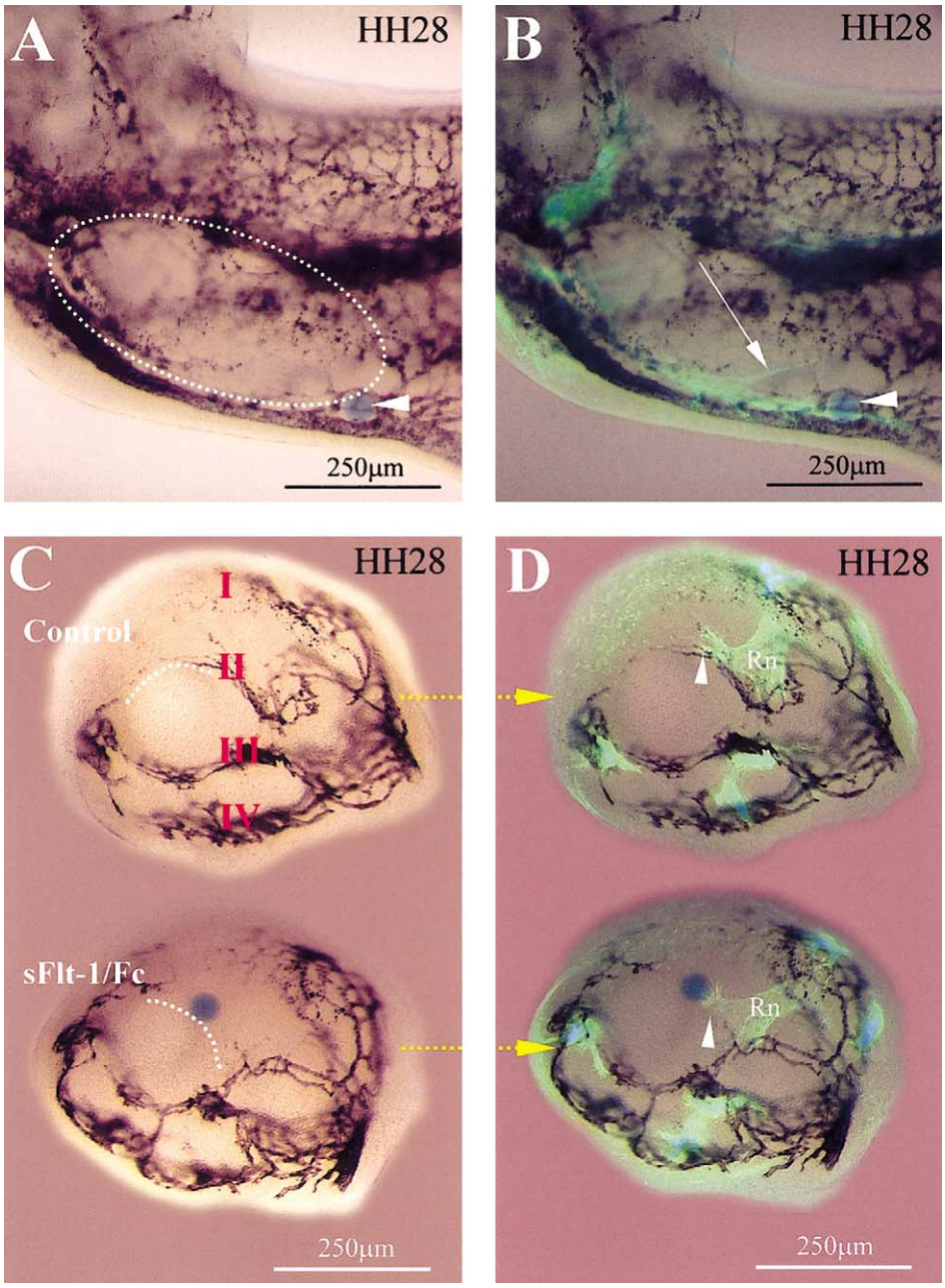

Fig. 4. Forelimb hypovascularization did not alter the forelimb peripheral nerve pattern. The forelimb specimens in the right-hand column correspond to those on the left, but with peripheral nerves (green) superimposed. (A) Ventral whole-mount view of an E5.5 (HH28) forelimb into which a sFlt-1/Fc-soaked bead has been implanted (arrowhead). Both capillaries and arteries (black) failed to form (area enclosed by dotted ellipse). (B) Despite the absence of capillary layer III and the ulnar artery with which the cranial branch of the ulnar nerve usually tracks, the cranial branch of the ulnar nerve maintained a normal trajectory by diverging from its caudal branch (arrow). (C) Coronal section of an E5.5 forelimb into which a sFlt-1/Fc-soaked bead has been implanted (blue bead). The sFlt-1/Fc-soaked bead (bottom left) inhibited the formation of capillary layer II (compare with control specimen, top left). (D) Despite the absence of the capillary layer (arrowhead) on which the radial nerve (Rn) normally tracks, the Rn maintained a normal trajectory.

tion). If vascular smooth muscle was absent on forelimb blood vessels, along which nerves extend in vivo, this would not be consistent with the notion that vascular smooth muscle was an important determinant of forelimb neurovascular congruency. αSMA and NF-M double immunolabeling showed that nerves were closely associated with vascular smooth muscle surrounding forelimb blood vessels at E7 (HH32) (Fig. 1A); however, during nerve in-growth at E5 (HH26), αSMA immunoreactivity was confined to the dermomyotome and proximal brachial artery and was not associated with the other forelimb blood vessels along which nerves track (Fig. 1B). Hence, early congruent neurovascular spatial relationships were unlikely to arise from an effect of vascular smooth muscle on in-growing nerves.

QH-1 and NF-M double immunolabeling of sectioned E5

quail forelimbs demonstrated the endothelium of lumenized blood vessels along which nerves track (Fig. 1C and D). Four discrete layers of endothelial cells that form capillaries in stereotypic positions in the D-V axis of the forelimb were well defined despite other cells (e.g., hematopoietic cells) also being labeled. Furthermore, nerves appeared to have a close spatial relationship to the endothelial cells that formed lumenized blood vessels by fluorescence microscopy. To determine whether nerves use these endothelial cells as a direct substrate along which to extend, we performed transmission electron microscopy on five E5.5 (HH27–HH28) forelimbs. Coronal sections demonstrated that even the largest forelimb blood vessels (e.g., median artery) did not appear to have a basal lamina and were comprised of a single layer of endothelial cells (data not shown). Sagittal sections showed that nerves were several cell diameters (5–20 μm) away from the endothelial cell layer along which they appeared to track (Fig. 1E). Furthermore, the more distal nerve growth cones appeared to diverge even further from the endothelial cell layer.

Forelimb vascular pattern develops normally in the absence of nerves

To investigate whether nerves determine the forelimb vascular pattern, we performed 101 neural tube excisions. To completely remove forelimb nerves, neural tubes were excised from embryos of less than 19 somites from somite 12 to presumptive somite 23. The results of these experiments are summarized in Table 1.

Of the 101 embryos which underwent neural tube excision, 20 forelimbs had either no or a gross reduction in the number of nerves. The vascular pattern was analyzed at three separate time points and was normal in all aneural forelimbs.

Four E6 (HH29) totally aneural forelimbs were compared in detail with control limbs since, at this stage, most major forelimb arteries and veins have formed. In these limbs, both the arterial and venous blood vessels were located in the same positions as controls (Fig. 2A and B). The branches of these blood vessels were given off in the same location, sequence, and at the same time as control forelimbs. Furthermore, all blood vessels were found to be the same caliber as controls. For example, in all four aneural E6 forelimbs, the median artery was found to lie centrally and was parallel with the long axis of the limb. Consistent with the stage of development, the median artery divided distally into dorsal and ventral branches. The anterior and posterior marginal veins also formed normally along the pre- and postaxial forelimb margins, respectively. The capillary plexus was also found to be normal in aneural limbs. Avascular spaces in the autopod corresponding to the future digits formed in the same locations and in the same sequence as control limbs.

The vascular pattern in E8 (HH34) aneural forelimbs was also analyzed for two reasons. First, the adult vascular pattern is not fully established until E8 (Bates et al., 2002), so there was a possibility that further vascular development would not occur appropriately in the absence of nerves. Second, the small subset of blood vessels that appear to follow the trajectory of their corresponding nerves does not form until after E6. We reasoned that these blood vessels might be particularly susceptible to the absence of nerves for their formation and correct patterning. However, in the seven E8 forelimbs that did not contain any nerves, the blood vessel pattern was identical to controls (Fig. 2C and D) in the three spatial axes of the developing forelimb (Fig. 2C and D, insets).

We were also interested to see whether the absence of nerves might predispose to subsequent vascular regression. To address this question, we also analyzed two aneural forelimbs at E10 (HH36). In both forelimbs, vascular remodeling continued to occur. For example, as in control limbs, the ulnar artery became larger than the median artery and constituted the dominant arterial supply (Fig. 2E and F).

Forelimb nerve pattern develops normally despite alterations to the vascular pattern

We employed two different experimental strategies to determine whether the vascular pattern determines the developing forelimb nerve pattern in the quail embryo forelimb. The aim of both sets of experiments was to alter the vascular pattern. In the first series of experiments, the forelimb was made hypervascular by either increasing the size or the number of blood vessels. In the second series, we aimed to make the forelimb avascular. In both sets of experiments, the alteration to the vascular pattern was made focally and close to the trajectory of a future in-growing nerve. Beads were implanted into the developing forelimb prior to nerve in-growth. The results of the bead experiments are summarized in Table 2. In all 136 control bead implantations, both the peripheral nerve and blood vessel patterns were found to be normal (Fig. 3).

Hypervascular upper limbs have a normal peripheral nerve pattern

$VEGF_{164}$ and $VEGF_{165}$ yielded similar results and are treated together as $VEGF_{164/165}$. Fifteen of 24 (63%) forelimbs receiving beads soaked in $VEGF_{164/165}$ had focal increases in vascularity. The vascular changes included focal hemorrhage, blood vessel dilation, blood vessel deviation toward the bead, and neovascularization (i.e., new and ectopic blood vessel formation). In 12 of these 15 cases (80%), the nerve pattern was normal; the remaining three are discussed further below.

$VEGF_{121}$-soaked beads also produced changes in the vascular pattern that were similar to the changes induced by $VEGF_{164/165}$-soaked beads. Blood vessel pattern was similarly altered by Ang-1; however, the effect of Ang-1 alone was less than $VEGF_{164/165}$ alone. Hemorrhage was not seen in the $VEGF_{121}$- or Ang-1-treated limbs. Six of 9 (66%)

forelimbs receiving beads soaked in either human $VEGF_{121}$ or Ang-1 had focal increases in vascularity, none of which was associated with abnormalities in the forelimb nerve pattern. When $VEGF_{165}$ was combined with Ang-1, the effect on the vascular pattern was greater than $VEGF_{164/165}$ or Ang-1 alone (data not shown). Adjacent blood vessels appeared to undergo intercalation to form fewer, much larger blood vessels.

In hypervascularization bead experiments, blood vessels were often increased in number and directed toward the bead. Nerves did not deviate from their normal trajectories to accompany these aberrant blood vessels (Fig. 3B). Similarly, in those cases in which blood vessels were induced to grow in areas not normally vascularized (Fig. 3C and D), nerves did not use the neo-vessels as pathways along which to track.

In 4 of 19 cases (21%) in which bead implantation ($VEGF_{164/165}$ and $VEGF_{165}$ + Ang-1 groups combined) caused forelimb hypervascularization, nerve formation or trajectory was also found to be different to controls (Fig. 3E). In 3 of these cases, the bead appeared to be acting as a physical barrier to axon outgrowth (Fig. 3F), and in 1 case, a nerve branch appeared to be defasciculated in the vicinity of the bead (data not shown). In all of these cases, the changes in the forelimb nerve pattern were not spatially congruent with changes in the vascular pattern. Nerves in the remaining 15 hypervascularized forelimbs (79%) were not observed to be hypertrophic or defasciculated, and they followed the same pathways as in control limbs.

Hypovascular upper limbs have a normal peripheral nerve pattern

Seven of 15 (47%) forelimbs containing beads soaked in soluble human Flt-$1/F_c$ chimera protein (sFlt-1/Fc) had focal decreases in vascularity. Beads that were implanted in normally avascular regions of the forelimb could not be assessed. In 4 of 7 forelimbs, focal areas of hypo- and avascularity were present along the trajectory of a forelimb nerve. In all hypovascularization experiments, both the arteries and the capillary layers along which nerves normally track were affected.

Capillaries were found to be absent or decreased in number either proximal to or in the immediate vicinity of the bead (Fig. 4A). A decrease in the density of capillaries distal to a growing nerve did not result in a change in its trajectory (data not shown). Similarly, if the capillary layer along which a nerve normally tracked was absent, the nerve still maintained a normal trajectory (Fig. 4B–D). Forelimb nerve branches formed in the same location, at the same angle, and at the same developmental time as controls. Nerve development was not retarded, and the morphology of nerves traversing experimental avascular areas was normal.

Vascular factors have little effect on spinal axon outgrowth in vitro, but Sema3A is a negative regulator

To determine whether the proteins used in the bead implantation experiments directly affected peripheral nerve outgrowth, we cultured E2 (HH13) neural tubes (forelimb level) for 3 days in medium supplemented with these proteins. A total of 29 neural tubes was analyzed. No statistically significant differences in axon density were observed in any of the experimental groups. The mean length of outgrowing axons from neural tubes was significantly reduced in culture medium supplemented with Sema3A ($P = 0.05$). In contrast, mean axon length was increased (compared with controls) in those neural tubes cultured in medium supplemented with either NGF or $VEGF_{165}$; however, these increases were not statistically significant. Medium supplemented with Ang-1, sFlt-$1/F_c$, $VEGF_{121}$, or $VEGF_{165}$ + Ang-1 did not have a statistically significant effect on mean axon length in vitro.

Distribution of Sema3A immunoreactivity is consistent with negative regulation of neurovascular patterning

Frozen section immunolabeling of E6–E6.5 (HH29–HH30) forelimbs with Sema3A antibody was consistent with a negative regulation of neurovascular patterning (Fig. 5A–D). Sema3A was expressed between capillary layers I and II and between capillary layers III and IV. This distribution pattern matched the distribution of skeletal muscle by MF20 antibody frozen section immunolabeling (data not shown).

To determine whether the temporal expression pattern of Sema3A was consistent with negative regulation of neurovascular patterning, frozen section double immunolabeling was performed in E5 (HH26) forelimbs at the time of nerve in-growth. Sema3A protein was expressed proximally in the dermomyotome (Fig. 5E) but was absent distally at the level of the growing nerve front (Fig. 5F).

Sema3A misexpression is associated with abnormalities in both nerve and blood vessel patterning in the forelimb

We employed two different experimental strategies to determine whether Sema3A has a functional role in the determination of neurovascular pattern. In the first series of experiments, Sema3A-soaked beads were implanted into the developing forelimb at two time points: (1) prior to nerve in-growth at E4.5 (HH25); and (2) during nerve in-growth at E5 (HH26). In the second series of experiments, beads soaked in Sema3A antibody were implanted at E4.5. The results of these bead experiments have been combined in Table 2.

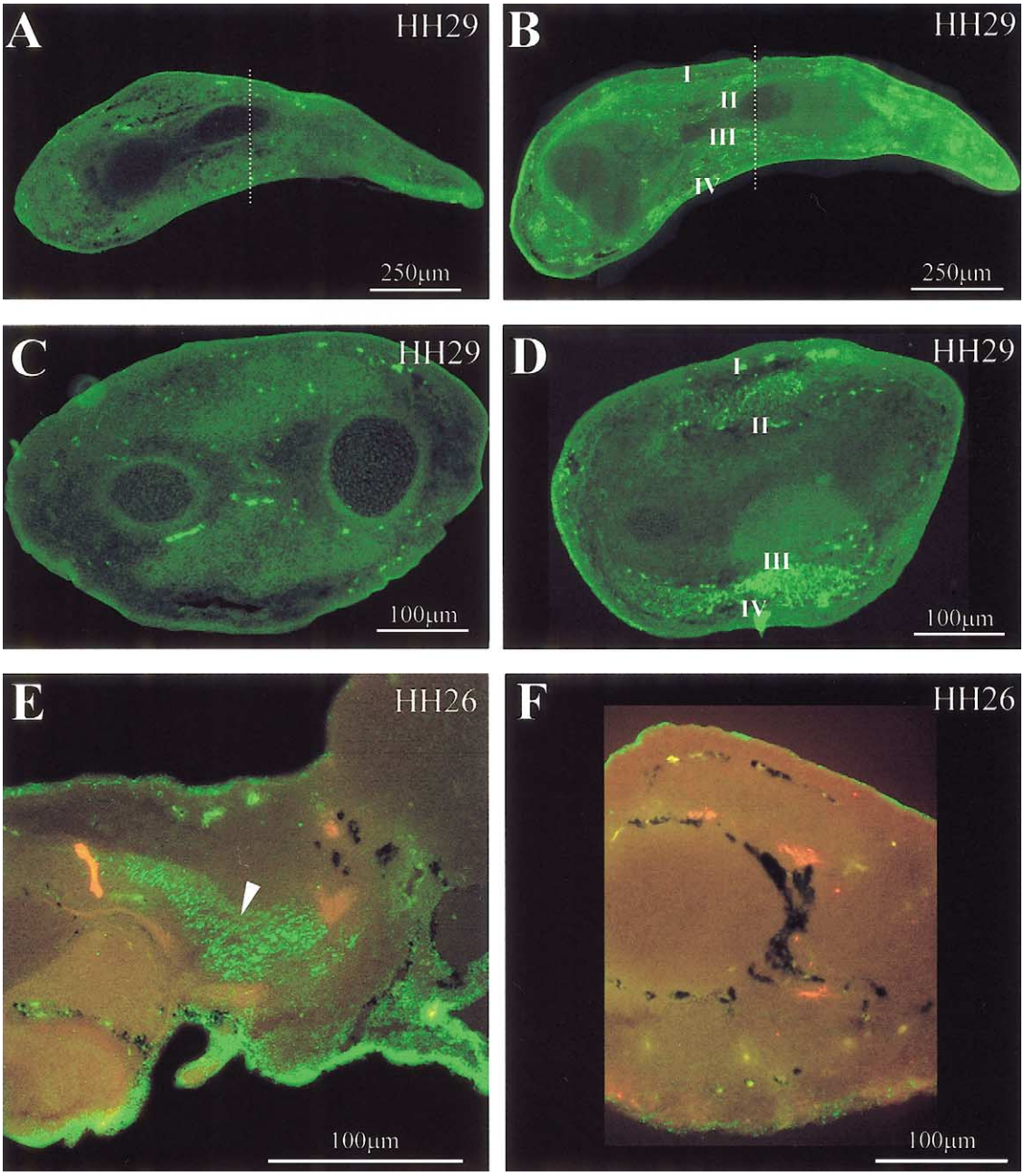

Fig. 5. Sema3A immunoreactivity was consistent with a negative regulation of neurovascular patterning. (A–D) Red blood cells autofluoresce within the four forelimb capillary layers. (A) Sagittal section of an E6.0 (HH29) control forelimb (no primary antibody). The vertical line indicates the plane of the coronal section shown in (C). (B) Sagittal section of an E6.0 forelimb immunolabeled with Sema3A antibody demonstrated immunoreactivity (green) between capillary layers I and II and between layers III and IV. The vertical line indicates the plane of the coronal section shown in (D). (C) E6.0 control coronal section. The diffuse green staining is background only. (D) Coronal section of an E6.0 forelimb immunolabeled with Sema3A antibody demonstrated a granular distribution pattern confined to the region between capillary layers I and II and between layers III and IV. (E). Sagittal section of an E5.0 (HH26) proximal forelimb showing Sema3A (green) and peripheral nerve (red) distribution patterns. Sema3A protein distribution was confined to the dermomyotome. Nerves were excluded from this region. (F) Coronal section of an E5 distal forelimb. Sema3A immunoreactivity was not present at the level of the growing nerve (red) front. Blood vessels are labeled black.

Ectopic Sema3A causes altered nerve patterns and hypovascularization in the developing forelimb

Three of five (60%) assessable forelimbs of embryos receiving Sema3A-soaked beads at E4.5 (HH25) had forelimb nerve and blood vessel distribution patterns that were different from controls (Fig. 6A). Nerve abnormalities included altered trajectories (Fig. 6B), deviation away from the bead (Fig. 6C and D), and failure of nerve branches to form (Fig. 6E and F). The width of major forelimb nerves (e.g., radial and median nerves) was also smaller than control limbs (data not shown).

Ectopic Sema3A also induced changes in the vascular

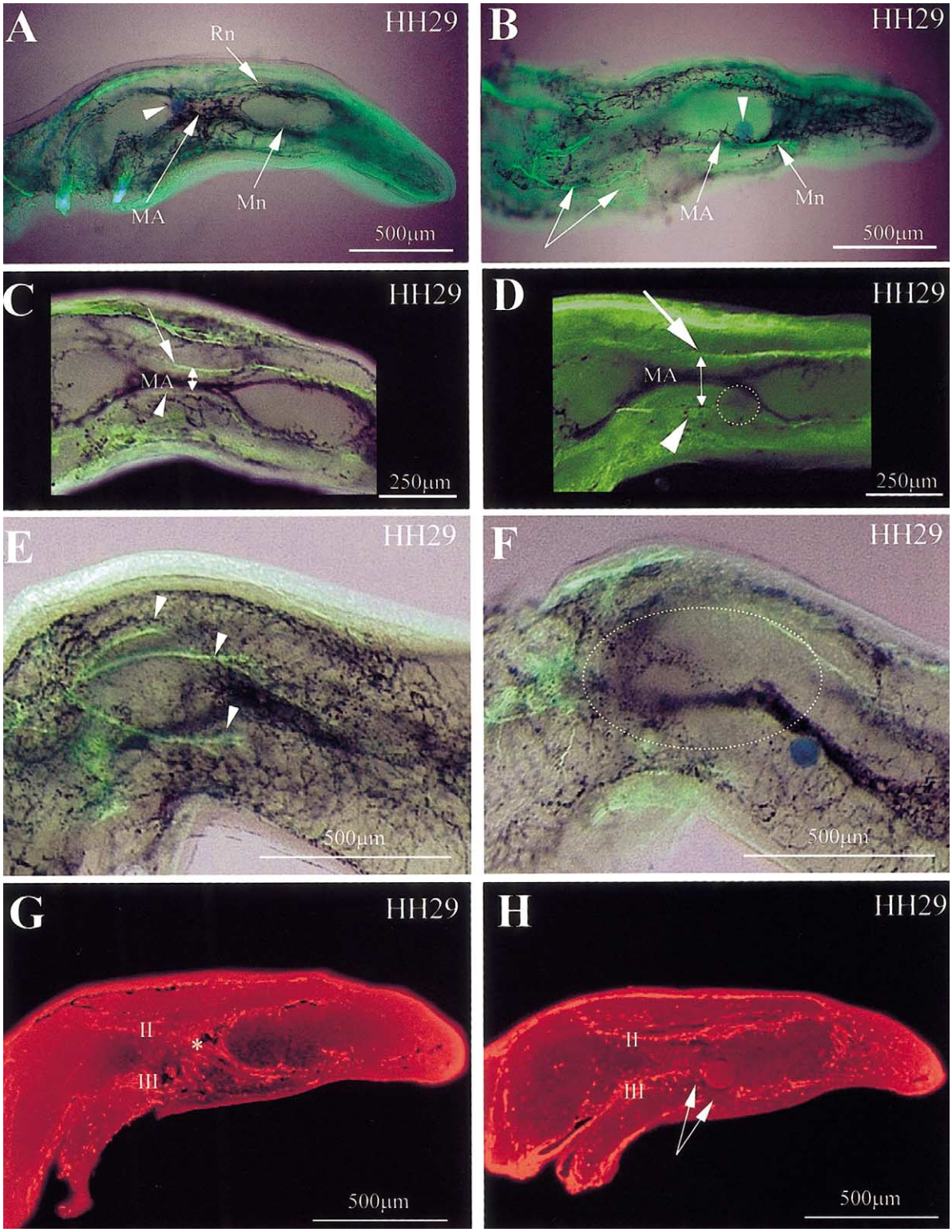

Fig. 6. Ectopic Sema3A protein in the developing forelimb caused abnormalities in neurovascular patterning. (A) Sagittal section of an E6 (HH29) control forelimb showing that the EGFP culture media-soaked bead (arrowhead) did not alter the trajectory of the radial (Rn) or median (Mn) nerves. (B) Sagittal section of an E6 forelimb into which a Sema3A-soaked bead has been implanted (arrowhead). The Mn deviated ventrally away from the bead, and ventral cutaneous nerves in the proximal part of the forelimb (arrows) showed an irregular trajectory. The MA was decreased in caliber. (C) Sagittal section of an E6 control forelimb showing the close spatial relationship between the Rn (arrow), the Mn (arrowhead), and the MA. The double-headed arrow indicates the normal distance between the Rn and Mn on either side of the MA. (D) Sagittal section of an E6 (HH29) forelimb implanted with a Sema3A-soaked bead (position indicated by dotted circle) showed abnormal deviation (indicated by longer double-headed arrow) of the Rn (arrow) and Mn (arrowhead) away from the MA (compare with C). (E) Dorsal whole-mount view showing the normal distribution of cutaneous nerves (arrowheads) and capillaries (black) in an E6

pattern that were spatially associated with nerve abnormalities. Vascular abnormalities included a reduction (decrease in capillary density) or absence of the capillary layers along which forelimb nerves normally track (Fig. 6D and F). Major blood vessels (e.g., median artery) were reduced in caliber and deviated away from the bead. In some cases, blood vessels were replaced by a disorganized array of endothelial cells revealed by QH-1 antibody immunolabeling (data not shown).

Three of seven (43%) assessable forelimbs of embryos receiving Sema3A-soaked beads at E5 (HH26) had subtle changes in the forelimb nerve pattern. Nerves deviated away from the bead but assumed a normal trajectory further distally (data not shown). In contrast to the subtle changes in the nerve pattern, changes in the vascular pattern were as profound as those observed in the E4.5 Sema3A bead implantations. Blood vessels were again reduced in caliber or were absent and replaced by a disorganized array of endothelial cells (Fig. 6G and H).

Ectopic Sema3A antibody causes forelimb hypervascularization without a change in the peripheral nerve pattern

Two of three assessable forelimbs of embryos receiving Sema3A antibody-soaked beads at E4.5 (HH25) caused significant changes to the developing vascular pattern compared with controls (Fig. 7A). Abnormalities in the vascular pattern were not associated with changes in the forelimb nerve pattern or nerve defasciculation (data not shown). Capillaries surrounding and proximal to the bead were disorganized, dilated, and converged toward the bead (Fig. 7B). Blood vessels were also found to grow toward and around the bead in normally avascular spaces, and there was a contraction of the space between capillary layers I and II (Fig. 7C and D).

Electroporation of sNRP1 in neural derivatives causes abnormalities in the formation and patterning of nerves and blood vessels in the forelimb

The neural tubes of 46 E2 (HH13) quail embryos were electroporated with cDNA constructs for sNRP1 and EGFP (sNRP1 + GFP). Thirty-six neural tubes were electroporated with EGFP constructs alone and served as controls. Of the 23 sNRP1/GFP electroporated embryos that survived to E5–E6 (HH26–HH29), 22 (96%) expressed EGFP in the neural tube opposite the forelimb at E3 (HH20). Seven of 22 (32%) were found to have significant abnormalities in neurovascular development and pattern formation. In contrast, there were no neurovascular abnormalities in the 13 control GFP-positive embryos surviving to E6. These results are summarized in Table 3.

In some cases, forelimb nerves were defasciculated (Fig. 8A and B), and in others, there was a severe disruption in the peripheral nerve pattern. For example, brachialis longus inferior and brachialis longus superior joined proximally in the forelimb to give rise to an aberrant preaxial nerve branch not seen in controls (Fig. 8E and F). In other cases, abnormal peripheral nerve branches could not be identified by standard nomenclature.

Abnormalities in the vascular pattern accompanied the abnormalities in the peripheral nerve pattern. In some cases, changes to the neurovascular patterns were congruent (Fig. 8C and D), and in others, they were not (data not shown). Changes to the vascular pattern included ectopic blood vessels that were interconnected in an abnormal configuration that resembled a vascular malformation (Upton et al., 1999). In other cases, blood vessels appeared to be dilated to form a punctate globular pattern and were associated with extravasation of blood into the limb mesenchyme (Fig. 8G). In one case, an ectopic digit formed on the preaxial border of the forelimb (data not shown).

Discussion

Nerve and blood vessel anatomical patterns in the forelimb of vertebrate adults are branching, complex, stereotypic, and highly conserved in vertebrates (Coleman and Anson, 1961; Mackinnon and Dellon, 1988; Taylor et al., 1994; Taylor and Minabe, 1992). These patterns are established during embryogenesis (see Introduction). We have previously examined in detail the nerve and blood vessel pattern in over 1600 whole-mount quail embryo forelimbs from E2 to E15 (HH13–HH41) (Bates et al., 2002). Peripheral nerves were always found to track on one of four capillary layers in the D-V axis of the forelimb. These capillary layers were composed only of endothelium, and as patent vessels, could be best appreciated with India Ink injection and examination in whole mount (Bates et al., 2002). These capillary layers were present in the forelimb prior to nerve in-growth, and the timing and spatial relationship were consistent with the nerves using these capillaries as a scaffold along which to extend. Furthermore, neurovascular congruency has also been observed in the A-P and P-D axes of the developing forelimb (Bates et al., 2002). The leading axons of forelimb nerves (e.g., median nerve) extended along and around the largest blood vessels (e.g., median artery) in the A-P axis. However, in certain

control specimen. (F) Dorsal whole-mount view showing the effect of a Sema3A-soaked bead on peripheral nerve and blood vessel formation (area enclosed by dotted circle). Cutaneous nerves and capillaries failed to form. (G) Sagittal section of an E6 control specimen immunolabeled with QH-1 (red) to reveal the distribution and organization of endothelial cells. Capillary layers II and III converged to form the large median artery (asterisk) in the center of the forelimb. (H) Implantation of Sema3A-soaked beads at E5 caused decreased capillary tube formation (arrows) and a disorganized distribution of endothelial cells. Capillary layers II and III did not converge to form the MA.

cases (see below), discrete nerves foreshadowed the course of blood vessels. These spatiotemporal relationships are consistent with nerves acting as guides for angiogenesis in certain cases, while in most cases, the blood vessels appear to act as guides for nerve extension.

As a technical note, there are several markers for avian vascular cells (Herzog et al., 2001; Labastie, 1989; Peault et al., 1983; Wilting et al., 1997). QH-1 is an antibody marker of quail endothelial and hematopoietic cells (Pardanaud et al., 1987) and periderm (Brand-Saberi et al., 1995). However, QH-1 immunoreactivity is not restricted to lumenized vessels in the forelimb of the quail embryo. Hence, whole-mount immunolabeling with QH-1 does not facilitate analysis of the pattern of lumenized blood vessels in the forelimb because of diffuse fluorescence due to the large number of cells labeled outside the lumenized vessels (data not shown). However, frozen section immunolabeling with QH-1 was able to demonstrate the four discrete layers of endothelial cells that form capillaries in stereotypic positions in the D-V axis of the forelimb (Bates et al., 2002).

Nerves do not guide the development of the vascular pattern

In most cases, blood vessels occupy stereotypic positions in the forelimb before nerves but there are several exceptions to this rule (e.g., the cranial branch of the ulnar nerve). The adult quail vascular pattern is established in the embryo at E8 (HH34) but undergoes differential remodeling events (e.g., changes in the caliber of blood vessels) such that, by E10 (HH36), the ulnar artery has replaced the median artery as the dominant (largest) limb forelimb blood vessel. This remodeling occurs in the presence of preexisting nerves adjacent to the blood vessels. In their study of neurovascular relationships in the skin, Martin et al. (1989) and Mukouyama et al. (2002) suggested that peripheral nerves may (1) induce certain vessels to form and/or (2) modify existing vascular patterns. Mukouyama et al. (2002) suggest that peripheral sensory nerves are required for the differentiation of small-diameter skin arteries, but evidence supporting a role for nerves in the determination of vascular patterning in major axial vessels is much less convincing. This study did not examine the pattern of major axial blood vessels (where we have observed the highest degree of neurovascular congruency) in either the ErbB3 or the Neurogenin1/Neurogenin2 knockout mice on which their conclusions are based. Furthermore, without specifically knocking out the ErbB3 gene in Schwann cells, quantifying changes in VEGF expression in ErbB3 mutants and analyzing cocultures of ErbB3$^{-/-}$ endothelial cells with wild type dorsal root ganglia (and vice versa) in terms of their ability to differentiate, it is difficult to ascertain whether the changes in vascular pattern observed in their study are directly attributable to changes in the peripheral nerve pattern.

To address the question of whether nerves are required for the formation of a normal vascular pattern (i.e., capillary layers and major named axial vessels), we analyzed the vascular pattern in aneural quail forelimbs at three separate time points (E6, E8, and E10). In all cases, the vascular pattern was found to be normal in the absence of nerves. Major arteries and veins were found in the same positions as controls, and vascular branches formed in the correct sequence, at the correct time, and in correct locations. In particular, those blood vessels that appeared to follow the trajectory of a nerve formed normally in the absence of that nerve. Capillary layers were formed normally, and avascular spaces were indistinguishable from controls. Furthermore, differential vascular remodeling proceeded normally up to E10 in the absence of forelimb nerves. Hence, we conclude that nerves are not required for the formation of a normal vascular pattern, nor for the later remodeling events that produce the adult pattern in the quail forelimb.

Blood vessels do not guide the development of the peripheral nerve pattern

In-growing nerves do not physically contact vascular smooth muscle or endothelium

In contrast to the vertebrate embryo, all blood vessels in the vertebrate adult are lined by endothelium and, except for capillaries, are surrounded by one or more layers of smooth muscle cells (DeRuiter et al., 1997). The lining of forelimb blood vessels with vascular smooth muscle commences in a P-D direction (Takahashi et al., 1996). The timing of this event is poorly characterized in avian embryos (Drushel et al., 1985; Vargesson and Laufer, 2001) but appears to occur around E5 (HH26), well after the earliest forelimb blood vessels have formed at E2.5 (HH17). Hence, vascular smooth muscle is a poor marker of early forelimb vasculature. Nerve in-growth also occurs relatively late during forelimb development (see Introduction), and it is not known whether the appearance of vascular smooth muscle provides the earliest in-growing axons with a favorable substrate on which to grow. To determine whether vascular smooth muscle might normally support the nerve outgrowth in vivo, we performed double fluorescent immunolabeling for αSMA (vascular smooth muscle) and NF-M (peripheral nerves). Spatiotemporal analysis of vascular smooth muscle and nerve distribution in quail embryo forelimbs did not support the hypothesis that peripheral nerves initially track along blood vessels because of the presence of vascular smooth muscle. The in-growing nerve front was found to lie distal to the distribution of vascular smooth muscle at E5–E5.5 (HH27–HH29). For example, the radial and ulnar nerves tracked along blood vessels that did not contain any vascular smooth muscle in their walls by αSMA immunoreactivity. We conclude that vascular smooth muscle is not a prerequisite for initial axon outgrowth in vivo.

Endothelium (QH-1) and NF-M double immunolabeling suggested a close spatial relationship between all forelimb nerves and endothelial cell-lined blood vessels during the period of nerve in-growth and pattern formation (E3.5–E8).

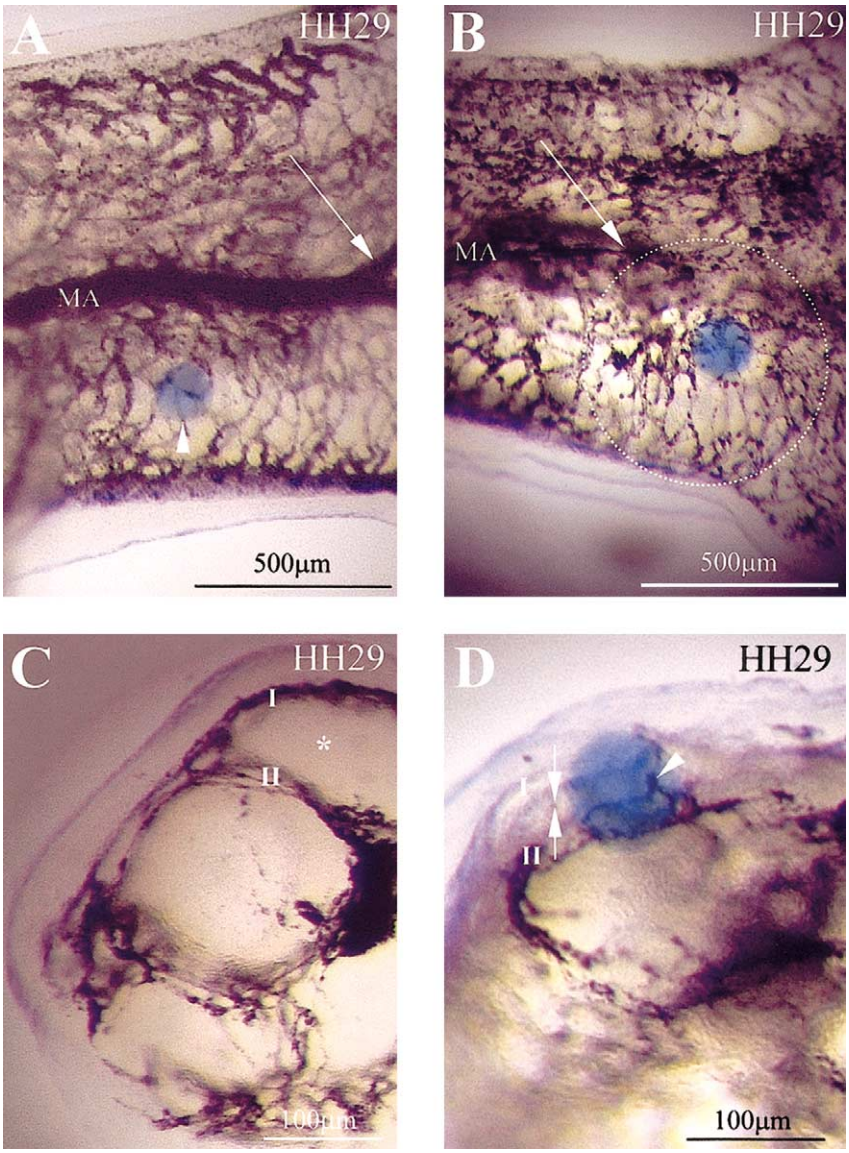

Fig. 7. Ectopic Sema3A antibody in the developing forelimb caused abnormalities in vascular patterning. (A) Dorsal whole-mount of an E6 (HH29) forelimb implanted with a PBS control bead (arrowhead points to bead). This did not alter the trajectory of the median artery (MA) or the size of its dorsal branch (arrow). (B) Dorsal whole-mount of an E6 (HH29) forelimb into which a Sema3A antibody-soaked bead has been implanted. Capillaries (black) surrounding the bead (enclosed by dotted circle) were dilated, disorganized, and appeared to converge on the bead. The dorsal branch of the median artery (arrow) is smaller than the control limb and has an aberrant trajectory. (C) Coronal section of an E6 control forelimb showing capillary layers I and II normally enclosing a large avascular space (asterisk). (D) Coronal section of an E6 forelimb into which a Sema3A antibody-soaked bead has been implanted showing capillaries converging around the bead (arrowhead) and convergence of capillary layers I and II (arrows) that appeared to obliterate the normally avascular space between these two layers.

Table 3
sNRP1 neural tube electroporation results

	Total no. experiments	Alive at E5–E6 (HH26–HH29)	GFP + ve[a]	Abnormal vessels and/or abnormal nerves[b]	Normal vessels and normal nerves[b]
GFP only control	36	16	13	0	13
sNRP1 + GFP	46	23	22	7	15
Total	82	39	35	7	28

[a] Number of embryos alive at E5 that were also GFP + ve at E3 (HH20).
[b] Forelimb neurovascular analysis was only performed on GFP + ve embryos.

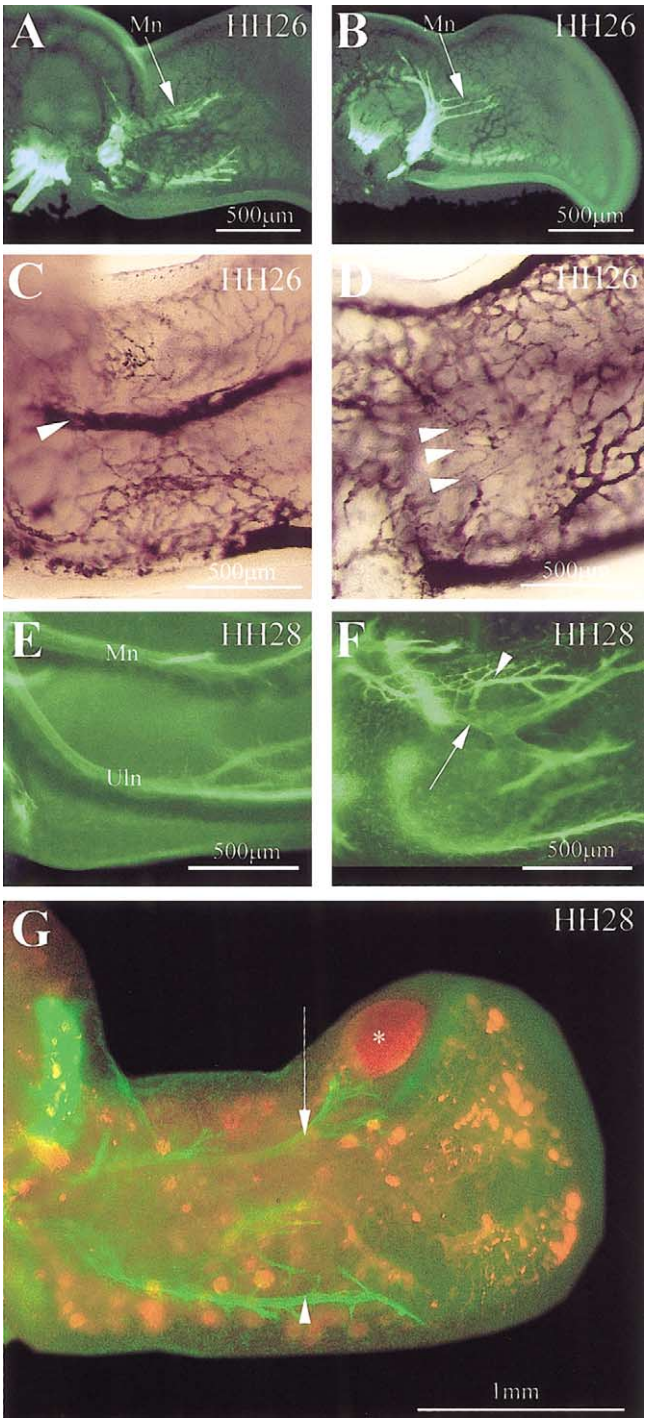

Fig. 8. Overexpression of sNRP1 in the neural tube was associated with abnormalities in both forelimb peripheral nerve and blood vessel formation and patterning. All images are ventral whole mounts. (A) E5 (HH26) control forelimb showing the normal morphology of the median nerve (Mn). (B) E5 forelimb electroporated with sNRP1 showing defasciculation of the Mn. This change in peripheral nerve pattern was spatially congruent with the median artery trifurcation seen in (D). (C) E5 control forelimb showing the normal morphology of the median artery (arrowheads). (D) E5 forelimb electroporated with sNRPI. The median artery divided abnormally into three separate branches (multiple arrowheads) at its origin. (E) E5.5 (HH28) control forelimb showing the normal morphology of the median (Mn) and ulnar (Uln) nerves in the proximal forelimb. (F) E5.5 forelimb electroporated with sNRP1 was associated with an abnormal communication between the brachialis longus superior and inferior nerves (arrow) and aberrant cutaneous nerve branches (arrowhead). (G) E5.5 forelimb electroporated with sNRP1 was associated with profound abnormalities in neurovascular development and patterning. The Uln (arrowhead) branched abnormally along the postaxial border of the forelimb. A preaxial nerve branch (arrow) formed that has no counterpart in normal forelimbs. Vascular abnormalities included multiple vessel dilations and hemorrhage (asterisk).

Endothelial cells formed well-defined capillary layers along which nerves appeared to extend. We therefore performed TEM at E5.5 (HH29) to clarify the physical relationship between in-growing nerves and endothelial cells in the forelimb of the quail embryo. Forelimb nerves were located 5-20 μm away from the endothelial cell layer along which they appeared to extend by light microscopy. The nerve growth cones appeared to diverge from the endothelial layer as they progressed distally into the forelimb. These findings are consistent with the observation of Tosney et al. (1985) that the intersomitic blood vessels lie 30–40 μm anterior to the spinal nerve pathway. Furthermore, our finding that blood vessels were composed of a single layer of endothelial cells lacking a basal lamina was also consistent with earlier studies (Caplan, 1985; Drushel et al., 1985). In agreement with Tosney et al. (1985), the hypothesis that blood vessels or their basal lamina ECM were providing a direct substrate for peripheral nerve outgrowth and patterning was not supported by our results. The possibility that the vasculature influenced the peripheral nerve pattern by providing diffusible guidance cues, trophic factors, or more distant ECM remained to be excluded.

Alteration of vascular pattern does not alter nerve pattern

To determine whether the vasculature influenced the peripheral nerve pattern by providing diffusible guidance cues, distant ECM or trophic factors, we focally altered the vascular pattern prior to peripheral nerve in-growth to that region. $VEGF_{165}$, $VEGF_{121}$, and Ang-1-soaked beads caused increases in vascular density, increases in blood vessel size, blood vessel deviation toward the bead, and neovascularization in all regions of the developing forelimb. These findings are consistent with studies that observed the formation of supernumerary blood vessels in normally avascular regions after vascular growth factor application (Drake and Little, 1995; Flamme et al., 1995; Suri et al., 1998; Wilting et al., 1996; Yin and Pacifici, 2001). In contrast, other studies have shown that overexpression of vascular growth factors is only associated with increases in vascular density, diameter, and permeability in permissive areas (regions that are vascularized during normal development) (Flamme et al., 1995; Suri et al., 1998). We find that, although neovascularization can be induced by vascular growth factors in all forelimb regions (including avascular regions), there exists a spatial hierarchy of permissiveness. Neovascularization occurs most readily in normally vascularized areas, less readily in the regions between capillary layers I and II and between capillary layers III and IV

(dorsal and ventral muscle masses, respectively), and least readily between capillary layers II and III (prechondrogenic mesenchyme).

Despite significant alterations to the vascular pattern, the majority of in-growing forelimb nerves did not change their trajectory to accompany aberrant blood vessels. Thus, blood vessels did not appear in general to be guiding nerves or providing them with an alternative pathway on which to track. In four cases, the pattern of peripheral nerves was observed to change. In these cases, the changes in peripheral nerve trajectory were not spatially congruent with changes in the vascular pattern, and the bead appeared to be physically obstructing nerve outgrowth. However, the possibility that $VEGF_{165}$ was acting directly on forelimb nerves (Jin et al., 2000; Sondell et al., 1999a, 1999b, 2000) remained to be excluded (see below).

The soluble form of flt-1 (VEGF receptor 1) is a potent antagonist of VEGF signaling (Chen et al., 2000; Kendall and Thomas, 1993) and vasculogenesis (Drake et al., 2000). Bead experiments with sFlt-1/F_c significantly decreased or abolished the formation of capillary layers or specific arteries. Capillaries were reduced in number immediately surrounding and proximal (in the region of draining veins) to the bead. Despite absence of the capillary scaffold upon which nerves were observed to track, the forelimb nerve pattern remained normal and the morphology of nerves was the same as control specimens. The simplest conclusion from these results is that the vasculature does not determine forelimb nerve pattern.

Molecular evidence is consistent with the possibility that changes to the forelimb nerve pattern seen in association with $VEGF_{165}$ bead application in this study could be due to a direct effect of $VEGF_{165}$ on these nerves. Recent studies have suggested that $VEGF_{165}$ has neurotrophic effects in vitro (Jin et al., 2000; Sondell et al., 1999a, 2000) and in vivo (Schratzberger et al., 2000, 2001; Sondell et al., 1999b). $VEGF_{165}$ binds to both NRP-1 and flk-1 and both of these receptors are present on nerves (Sondell et al., 1999a,b; Takagi et al., 1987). Although some studies suggest that the neurotrophic effects of $VEGF_{165}$ are mediated through the flk-1 receptor directly (Jin et al., 2000; Sondell et al., 1999a, 2000), evidence also points to the NRP1 receptor. To determine whether changes to the peripheral nerve pattern in a few of our hypervascularization experiments with $VEGF_{165}$ (see above) may be attributable to a direct neurotrophic effect, we performed neural tube cultures supplemented with $VEGF_{165}$, $VEGF_{121}$, Ang-1, and $VEGF_{165}$/Ang-1 combined. Effects of $VEGF_{165}$ on mean axon length was not significantly different from controls ($P = 0.27$). Our results suggest that the changes in forelimb nerve pattern seen in a few cases with $VEGF_{165}$ in vivo were not due to a direct effect of $VEGF_{165}$ on peripheral nerves. Differences in the experimental model, $VEGF_{165}$ concentration, and in the method of axon length measurement may account for the different results seen in other studies.

The congruency of nerve and vascular anatomical pattern depends on similar molecular mechanisms that underlie the patterning of both tissues

Our results are not consistent with the hypothesis that neurovascular congruency arises from interdependence between nerves and blood vessels. This suggests that neurovascular pattern (and by default, neurovascular congruency) may arise by shared patterning mechanisms. Forelimb nerves and blood vessels avoid cartilage, muscle, and the subectodermal avascular zone in the developing forelimb; therefore, these hypothesized shared patterning mechanisms may include elements that negatively regulate peripheral nerve and blood vessel growth.

Sema3A has been shown to negatively regulate axonal and endothelial cell outgrowth in vitro (see Introduction). Consistent with previous studies describing the distribution of Sema3A mRNA (Giger et al., 1996; Wright et al., 1995), we find that at E6–E6.5 (HH29–HH30), Sema3A protein is found in regions (e.g., dorsal and ventral muscle masses) where forelimb nerves and blood vessels are absent. However, simultaneous analysis of Sema3A protein and peripheral nerve distribution during the early stages of nerve in-growth at E5 (HH26) reveal that Sema3A protein was first seen proximal to (i.e., behind) the growing nerve front. This is consistent with the notion that Sema3A acts via negative regulation to maintain neurovascular patterns already established, but is not consistent with Sema3A negatively regulating pathfinding by the first axons (Eickholt et al., 1999; Giger et al., 1996; Wright et al., 1995). However, the latter possibility cannot be entirely dismissed since the earliest functional but low-level Sema3A protein expression may have been undetectable in this study.

Consistent with the fact that both peripheral nerves and endothelial cells express the NRP1 receptor (Fujisawa et al., 1997; Herzog et al., 2001; Soker, 2001; Soker et al., 1998; Takagi et al., 1987), Sema3A bead experiments were found to profoundly affect neurovascular patterning and development in the quail forelimb in vivo. These findings are consistent with in vitro studies of growth cone behavior in the vicinity of Sema3A-soaked beads (Fan and Raper, 1995). Nerve abnormalites were observed to be more severe (e.g., failure of formation) in those forelimbs in which Sema3A-soaked beads were implanted prior to peripheral nerve in-growth at E4.5 (HH25) than in the vicinity of peripheral nerves at E5 (HH26). In contrast to the temporally variable severity of the effect of Sema3A on forelimb nerve patterning, endothelial cells appeared to be sensitive to Sema3A at both time points examined. Sema3A has been shown to inhibit capillary sprouting and endothelial motility in vitro (Miao et al., 1999) and our in vivo results are consistent with the notion that endothelial cells remain sensitive to Sema3A during the period of ongoing vascular remodeling that continues until E10 (HH36) (Bates et al., 2002). In contrast, the peripheral nerve pattern appears to be established with a high degree of precision ab initio (Hol-

lyday, 1990) and the adult nerve pattern is laid down by E6.5 (HH30) (Swanson and Lewis, 1982).

Sema3A knockout studies (Taniguchi et al., 1997) demonstrate increased peripheral nerve branching and altered nerve trajectories (into cartilage forming areas) that were not seen with our Sema3A antibody bead experiments. These differences may be due to low Sema3A antibody levels, lack of antibody specificity, and persistent Sema3A expression in our experimental forelimbs. Despite no observed change in the nerve pattern, Sema3A antibody-soaked beads caused blood vessel dilation and changes in the forelimb vascular pattern. Blood vessels were found to grow toward and around the bead in normally avascular spaces. This may reflect differences in nerve and endothelial sensitivity to changes in the level of molecules, such as Sema3A, that are involved in neurovascular patterning. The forelimb vascular pattern has not been examined in detail in Sema3A knockout mice, but overexpression of the transmembrane form of NRP1 in mice is associated with excess capillary formation, blood vessel dilation, and hemorrhage (Kitsukawa et al., 1995). In models of nerve regeneration, Sema3A mRNA is initially down-regulated, and then, following target reinnervation, normal expression levels are restored to maintain the neuronal network (Pasterkamp and Verhaagen, 2001). Our results are also consistent with the notion that Sema3A maintains and refines an established neurovascular pattern rather than initially defining it (see above).

sNRP1 is a truncated form of the NRP1 transmembrane receptor containing just the extracellular domains of this molecule (Gagnon et al., 2000; Rossignol et al., 2000). sNRP1 binds to both $VEGF_{165}$ (but not $VEGF_{121}$) and Sema3A (Gagnon et al., 2000). Monomeric sNRP1 inhibits and dimeric sNRP1 enhances vascular development in vitro (Yamada et al., 2001). Overexpression of sNRP1 in prostate tumor cells in vivo caused decreased vascularity, hemorrhage, and vascular disruption (Gagnon et al., 2000).

In our study, sNRP1 overexpression was associated with alterations to both nerve and vascular patterns during forelimb development. Forelimb nerves were defasciculated and had altered trajectories that resembled the defects seen in Sema3A knockout (Taniguchi et al., 1997) and NRP1 overexpression (Kitsukawa et al., 1995) studies in mice. sNRP1 overexpression was also associated with hemorrhage and ectopic, abnormally formed blood vessels that resembled vascular malformations. These findings also resembled those seen in the NRP1 overexpression studies (Kitsukawa et al., 1995). We did not observe the formation of avascular spaces and defective capillary formation that was seen in NRP1/NRP2 double knockouts (Takashima et al., 2002). sNRP1 has been shown to inhibit $VEGF_{165}$ activity in vitro (Gagnon et al., 2000); however, our sNRP1 overexpression results in vivo are suggestive of increased rather than decreased $VEGF_{165}$ activity (Drake and Little, 1995, 1999). It has been suggested that sNRP1 may form a dimer with NRP1-expressing cells, bind to $VEGF_{165}$, and then deliver $VEGF_{165}$ to NRP1-expressing endothelial cells (Yamada et al., 2001). This phenomenon may explain the phenotype observed in our study.

Conclusion

Neurovascular congruency observed between nerves and major axial blood vessels in the forelimb of the vertebrate embryo is established during embryogenesis. Peripheral nerves do not pattern these blood vessels, and blood vessels do not pattern these nerves. Rather, neurovascular congruency appears to be determined by a shared molecular patterning mechanism that involves Sema3A and NRP1. Sema3A appears to negatively regulate neurovascular patterning by stabilizing and maintaining established nerve and blood vessel networks. This system is under strict temporal control, and misexpression of either Sema3A or NRP1 early in development leads to profound disruptions to the forelimb neurovascular pattern.

Acknowledgments

We thank Marie-Aimee Teillet (Institut d'Embryologie du CNRS, France) for her advice on neural tube excision, Cheryll Tickle (Department of Cell and Developmental Biology, University of Dundee, Scotland) and Lee Niswander (Sloan-Kettering Institute, NY, USA) for their advice on forelimb bead implantation, Lynn Barnett (WEHI, Melbourne, Australia) for providing $VEGF_{165}$, and Steven Stacker (Ludwig Institute, Melbourne, Australia) for his kind advice and provision of $VEGF_{164}$, George Yancopoulos (Regeneron Pharmaceuticals Inc., NY, USA) for providing Ang-1, John Raper (Department of Neuroscience, University of Pennsylvania) for the chick Sema3A constructs and advice on its preparation, Cathy Krull and Mary Swartz (Developmental Neurobiology Lab, University of Missouri-Columbia, USA) for their advice on in ovo electroporation. We are also grateful to Simon Koblar (Department of Genetics, University of Adelaide, Australia) and Paul Whitington (Department of Anatomy and Cell Biology, University of Melbourne, Australia) for their valuable input. The Royal Australasian College of Surgeons, MCRI, Jack Brockhoff Foundation, and the Department of Surgery (Royal Melbourne Hospital, University of Melbourne) generously supported this work. The QH-1 and MF-20 monoclonal antibodies developed by F. Dieterlen-Lievre and D.A. Fischman, respectively, were obtained from the Developmental Studies Hybridoma Bank developed under the auspices of the NICHD and maintained by The University of Iowa, Department of Biological Sciences, Iowa City, IA 52242, USA.

References

Bagnard, D., Vaillant, C., Khuth, S.T., Dufay, N., Lohrum, M., Puschel, A.W., Belin, M.F., Bolz, J., Thomasset, N., 2001. Semaphorin 3A–vascular endothelial growth factor-165 balance mediates migration and apoptosis of neural progenitor cells by the recruitment of shared receptor. J. Neurosci. 21, 3332–3341.

Bates, D., Taylor, G., Newgreen, D., 2002. The pattern of neurovascular development in the forelimb of the quail embryo. Dev. Biol. 249, 300–320.

Behar, O., Golden, J., Mashimo, H., Schoen, F., Fishman, M., 1996. Semaphorin III is needed for normal patterning and growth of nerves, bones and heart. Nature 383, 525–528.

Bennett, M.R., Davey, D.F., Uebel, K.E., 1980. The growth of segmental nerves from the brachial myotomes into the proximal muscles of the chick forelimb during development. J. Comp. Neurol. 189, 335–357.

Borisov, A.B., Huang, S.K., Carlson, B.M., 2000. Remodeling of the vascular bed and progressive loss of capillaries in denervated skeletal muscle. Anat. Rec. 258, 292–304.

Brand-Saberi, B., Seifert, R., Grim, M., Wilting, J., Kuhlewein, M., Christ, B., 1995. Blood vessel formation in the avian limb bud involves angioblastic and angiotrophic growth. Dev. Dyn. 202, 181–194.

Caplan, A., 1985. The vasculature and limb development. Cell Differ. 16, 1–11.

Caplan, A., Koutroupas, S., 1973. The control of muscle and cartilage development in the chick limb: the role of differential vascularization. J. Embryol. Exp. Morphol. 29, 571–583.

Chen, H., Ikeda, U., Shimpo, M., Maeda, Y., Shibuya, M., Ozawa, K., Shimada, K., 2000. Inhibition of vascular endothelial growth factor activity by transfection with the soluble FLT-1 gene. J. Cardiovasc. Pharmacol. 36, 498–502.

Coleman, S., Anson, B., 1961. Arterial patterns in the hand based upon a series of 650 specimens. Surg. Gynecol. Obstet. 113, 409–424.

DeRuiter, M., Poelmann, R., VanMunsteren, J., Mironov, V., Markwald, R., Gittenberger-de-Groot, A., 1997. Embryonic endothelial cells transdifferentiate into mesenchymal cells expressing smooth muscle actins in vivo and in vitro. Circ. Res. 80, 444–451.

Drake, C.J., LaRue, A., Ferrara, N., Little, C.D., 2000. VEGF regulates cell behavior during vasculogenesis. Dev. Biol. 224, 178–188.

Drake, C., Little, C., 1995. Exogenous vascular endothelial growth factor induces malformed and hyperfused vessels during embryonic neovascularization. Proc. Natl. Acad. Sci. USA 92, 7657–7661.

Drake, C.J., Little, C.D., 1999. VEGF and vascular fusion: implications for normal and pathological vessels. J. Histochem. Cytochem. 47, 1351–1356.

Drushel, R., Pechak, D., Caplan, A., 1985. The anatomy, ultrastructure and fluid dynamics of the developing vasculature of the embryonic chick wing bud. Cell Differ. 16, 13–28.

Eickholt, B., Mackenzie, S., Graham, A., Walsh, F., Doherty, P., 1999. Evidence for collapsin-1 functioning in the control of neural crest migration in both trunk and hindbrain regions. Development 126, 2181–2189.

Enomoto, H., Crawford, P.A., Gorodinsky, A., Heuckeroth, R.O., Johnson Jr., E.M., Milbrandt, J., 2001. RET signaling is essential for migration, axonal growth and axon guidance of developing sympathetic neurons. Development 128, 3963–3974.

Fan, J., Raper, J., 1995. Localized collapsing cues can steer growth cones without inducing their full collapse. Neuron 14, 263–274.

Feig, S., Guillery, R., 2000. Corticothalamic axons contact blood vessels as well as nerve cells in the thalamus. Eur. J. Neurosci. 12, 2195–2198.

Feinberg, R.N., Latker, C.H., Beebe, D.C., 1986. Localised vascular regression during limb morphogenesis in the chicken embryo. I. Spatial and temporal changes in vascular pattern. Anat. Rec. 214, 405–409.

Flamme, I., Vonreuten, M., Drexler, H., Syedali, S., Risau, W., 1995. Overexpression of vascular endothelial growth factor in the avian embryo induces hypervascularization and increased vascular permeability without alterations of embryonic pattern formation. Dev. Biol. 171, 399–414.

Fujisawa, H., Kitsukawa, T., Kawakami, A., Takagi, S., Shimizu, M., Hirata, T., 1997. Roles of a neuronal cell-surface molecule, neuropilin, in nerve fiber fasciculation and guidance. Cell Tissue Res. 290, 465–470.

Gagliardini, V., Fankhauser, C., 1999. Semaphorin III can induce death in sensory neurons. Mol. Cell. Neurosci. 14, 301–316.

Gagnon, M.L., Bielenberg, D.R., Gechtman, Z., Miao, H.Q., Takashima, S., Soker, S., Klagsbrun, M., 2000. Identification of a natural soluble neuropilin-1 that binds vascular endothelial growth factor: in vivo expression and antitumor activity. Proc. Natl. Acad. Sci. USA 97, 2573–2578.

Giger, R.J., Wolfer, D.P., DeWit, G.M.J., Verhaagen, J., 1996. Anatomy of rat semaphorin III collapsin-1 mRNA expression and relationship to developing nerve tracts during neuroembryogenesis. J. Comp. Neurol. 375, 378–392.

Gu, X.H., Terenghi, G., Kangesu, T., Navsaria, H.A., Springall, D.R., Leigh, I.M., Green, C.J., Polak, J.M., 1995. Regeneration pattern of blood vessels and nerves in cultured keratinocyte grafts assessed by confocal laser scanning microscopy. Br. J. Dermatol. 132, 376–383.

Gupta, K., Kshirsagar, S., Li, W., Gui, L., Ramakrishnan, S., Gupta, P., Law, P., Hebbel, R., 1999. VEGF prevents apoptosis of human microvascular endothelial cells via opposing effects on MAPK/ERK and SAPK/JNK signaling. Exp. Cell Res. 247, 495–504.

Hallmann, R., Feinberg, R., Latker, C., Sasse, J., Rissau, W., 1987. Regression of blood vessels precedes cartilage differentiation during chick limb development. Differentiation 34, 98–105.

Hamburger, V., Hamilton, H., 1951. A series of normal stages in the development of the chick embryo. J. Morphol. 88, 49–92.

Herzog, Y., Kalcheim, C., Kahane, N., Reshef, R., Neufeld, G., 2001. Differential expression of neuropilin-1 and neuropilin-2 in arteries and veins. Mech. Dev. 109, 115–119.

Hobson, M.I., Brown, R., Green, C.J., Terenghi, G., 1997. Inter-relationships between angiogenesis and nerve regeneration: a histochemical study. Br. J. Plast. Surg. 50, 125–131.

Hollyday, M., 1990. Specificity of initial axonal projections to embryonic chick wing. J. Comp. Neurol. 302, 589–602.

Honma, Y., Araki, T., Gianino, S., Bruce, A., Heuckeroth, R., Johnson, E., Milbrandt, J., 2002. Artemin is a vascular-derived neurotropic factor for developing sympathetic neurons. Neuron 35, 267–282.

Inoue, T., Krumlauf, R., 2001. An impulse to the brain-using in vivo electroporation. Nat. Neurosci. 4, 1156–1158.

Itasaki, N., Bel-Vialar, S., Krumlauf, R., 1999. 'Shocking' developments in chick embryology: electroporation and in ovo gene expression. Nat. Cell Biol. 1, E203–E207.

Jin, K.L., Mao, X.O., Greenberg, D.A., 2000. Vascular endothelial growth factor: direct neuroprotective effect in in vitro ischemia. Proc. Natl. Acad. Sci. USA 97, 10242–10247.

Kawakami, A., Kitsukawa, T., Takagi, S., Fujisawa, H., 1996. Developmentally regulated expression of a cell surface protein, neuropilin, in the mouse nervous system. J. Neurobiol. 29, 1–17.

Kawasaki, T., Kitsukawa, T., Bekku, Y., Matsuda, Y., Sanbo, M., Yagi, T., Fujisawa, H., 1999. A requirement for neuropilin-1 in embryonic vessel formation. Development 126, 4895–4902.

Kendall, R., Thomas, K., 1993. Inhibition of vascular endothelial growth factor activity by endogenously encoded soluble receptor. Proc. Natl. Acad. Sci. USA 90, 10705–10709.

Kitsukawa, T., Shimizu, M., Sanbo, M., Hirata, T., Taniguchi, M., Bekku, Y., Yagi, T., Fujisawa, H., 1997. Neuropilin-semaphorin III/D-mediated chemorepulsive signals play a crucial role in peripheral nerve projection in mice. Neuron 19, 995–1005.

Kitsukawa, T., Shimono, A., Kawakami, A., Kondoh, H., Fujisawa, H., 1995. Overexpression of a membrane protein, neuropilin, in chimeric mice causes abnormalities in the cardiovascular system, nervous system and limbs. Development 121, 4309–4318.

Koch, M., Murrell, J.R., Hunter, D.D., Olson, P.F., Jin, W., Keene, D.R., Brunken, W.J., Burgeson, R.E., 2000. A novel member of the netrin family, beta-netrin, shares homology with the beta chain of laminin. Identification, expression, and functional characterization. J. Cell. Biol. 151, 221–234.

Labastie, M.C., 1989. MB1, a quail leukocyte-endothelium antigen: further characterization of soluble and cell-associated forms. Cell Differ. Dev. 27, 151–162.

Lengele, B., Dhem, A., 1989. Unusual variations of the vasculonervous elements of the human axilla. Report of three cases. Arch. Anat. Histol. Embryol. 72, 57–67.

Lewis, W., 1902. The development of the arm in man. Am. J. Anat. 1, 145–185.

Lucas, A., Stettenheim, P., 1972. Avian anatomy: integument, in: Handbook No. 362, United States Department of Agriculture, Washington D.C.

Luo, Y.L., Raible, D., Raper, J.A., 1993. Collapsin: a protein in brain that induces the collapse and paralysis of neuronal growth cones. Cell 75, 217–227.

Mackinnon, S., Dellon, A., 1988. Surgery of the Peripheral Nerve. Thieme Medical Publishers, Inc., New York.

Martin, P., Khan, A., Lewis, J., 1989. Cutaneous nerves of the embryonic chick wing do not develop in regions denuded of ectoderm. Development 106, 335–346.

Martin, P., Lewis, J., 1989. Origins of the neurovascular bundle: interactions between developing nerves and blood vessels in embryonic chick skin. Int. J. Dev. Biol. 33, 379–387.

Messersmith, E., Leonardo, E., Schatz, C., Tessier-Lavigne, M., Goodman, C., Kolodkin, A., 1995. Semaphorin III can function as a selective chemorepellent to pattern sensory projections in the spinal cord. Neuron 14, 949–959.

Miao, H.Q., Soker, S., Feiner, L., Alonso, J.L., Raper, J.A., Klagsbrun, M., 1999. Neuropilin-1 mediates collapsin-1/semaphorin III inhibition of endothelial cell motility: functional competition of collapsin-1 and vascular endothelial growth factor-165. J. Cell. Biol. 146, 233–241.

Miller, R., 1939. Observations upon the arrangement of the axillary artery and brachial plexus. Am. J. Anat. 64, 143–163.

Morales-Ruiz, M., Fulton, D., Sowa, G., Languino, L.R., Fujio, Y., Walsh, K., Sessa, W.C., 2000. Vascular endothelial growth factor-stimulated actin reorganization and migration of endothelial cells is regulated via the serine/threonine kinase Akt. Circ. Res. 86, 892–896.

Mukouyama, Y., Shin, D., Britsch, S., Taniguchi, M., Anderson, D., 2002. Sensory nerves determine the pattern of arterial differentiation and blood vessel branching in the skin. Cell 109, 693–705.

Newgreen, D.F., Minichiello, J., 1995. Control of epitheliomesenchymal transformation. I. Events in the onset of neural crest cell migration are separable and inducible by protein kinase inhibitors. Dev. Biol. 170, 91–101.

Noakes, P., Bennett, M., Stratford, J., 1988. Migration of Schwann cells and axons into developing chick forelimb muscles following removal of either the neural tube or the neural Crest. J. Comp. Neurol. 277, 214–233.

Ogunshola, O.O., Stewart, W.B., Mihalcik, V., Solli, T., Madri, J.A., Ment, L.R., 2000. Neuronal VEGF expression correlates with angiogenesis in postnatal developing rat brain. Brain Res. Dev. Brain Res. 119, 139–153.

Oosthuyse, B., Moons, L., Storkebaum, E., Beck, H., Nuyens, D., Brusselmans, K., Van Dorpe, J., Hellings, P., Gorselink, M., Heymans, S., Theilmeier, G., Dewerchin, M., Laudenbach, V., Vermylen, P., Raat, H., Acker, T., Vleminckx, V., Van Den Bosch, L., Cashman, N., Fujisawa, H., Drost, M.R., Sciot, R., Bruyninckx, F., Hicklin, D.J., Ince, C., Gressens, P., Lupu, F., Plate, K.H., Robberecht, W., Herbert, J. M., Collen, D., Carmeliet, P., 2001. Deletion of the hypoxia-response element in the vascular endothelial growth factor promoter causes motor neuron degeneration. Nat. Genet. 28, 131–138.

Pardanaud, L., Altmann, C., Kitos, P., Dieterlen-Lievre, F., Buck, C., 1987. Vasculogenesis in the early quail blastodisc as studied with a monoclonal antibody recognizing endothelial cells. Development 100, 339–349.

Pasterkamp, R.J., Verhaagen, J., 2001. Emerging roles for semaphorins in neural regeneration. Brain Res. Brain Res. Rev. 35, 36–54.

Peault, B., Thiery, J., Douarin, N.L., 1983. Surface marker for hemopoietic and endothelial cell lineages in quail that is defined by a monoclonal antibody. Proc. Natl. Acad. Sci. USA 80, 2976–2980.

Puschel, A., Adams, R., Betz, H., 1995. Murine semaphorin D/collapsin is a member of a diverse gene family and creates domains inhibitory for axonal extension. Neuron 14, 941–948.

Rohm, B., Ottemeyer, A., Lohrum, M., Pueschel Andreas, W., 2000. Plexin/neuropilin complexes mediate repulsion by the axonal guidance signal semaphorin 3A. Mech. Dev. 93, 95–104.

Rossignol, M., Gagnon, M.L., Klagsbrun, M., 2000. Genomic organization of human neuropilin-1 and neuropilin-2 genes: identification and distribution of splice variants and soluble isoforms. Genomics 70, 211–222.

Roush, W., 1998. Receptor links blood vessels, axons. Science 279, 2042.

Schratzberger, P., Schratzberger, G., Silver, M., Curry, C., Kearney, M., Magner, M., Alroy, J., Adelman, L.S., Weinberg, D.H., Ropper, A.H., Isner, J.M., 2000. Favorable effect of VEGF gene transfer on ischemic peripheral neuropathy. Nat. Med. 6, 405–413.

Schratzberger, P., Walter, D.H., Rittig, K., Bahlmann, F.H., Pola, R., Curry, C., Silver, M., Krainin, J.G., Weinberg, D.H., Ropper, A.H., Isner, J.M., 2001. Reversal of experimental diabetic neuropathy by VEGF gene transfer. J. Clin. Invest. 107, 1083–1092.

Shima, D.T., Mailhos, C., 2000. Vascular developmental biology: getting nervous. Curr. Opin. Genet. Dev. 10, 536–542.

Singer, E., 1933a. Embryological patterns persisting in the arteries of the arm. Anat. Rec. 55, 403–409.

Singer, E., 1933b. Human brachial plexus united into a single cord. Description and interpretation. Anat. Rec. 55, 411–419.

Soker, S., 2001. Neuropilin in the midst of cell migration and retraction. Int. J. Biochem. Cell Biol. 33, 433–437.

Soker, S., Takashima, S., Miao, H., Neufeld, G., Klagsbrun, M., 1998. Neuropilin-1 is expressed by endothelial and tumor cells as an isoform-specific receptor for vascular endothelial growth factor. Cell 92, 735–745.

Sondell, M., Lundborg, G., Kanje, M., 1999a. Vascular endothelial growth factor has neurotrophic activity and stimulates axonal outgrowth, enhancing cell survival and Schwann cell proliferation in the peripheral nervous system. J. Neurosci. 19, 5731–5740.

Sondell, M., Lundborg, G., Kanje, M., 1999b. Vascular endothelial growth factor stimulates Schwann cell invasion and neovascularization of acellular nerve grafts. Brain Res. 846, 219–228.

Sondell, M., Sundler, F., Kanje, M., 2000. Vascular endothelial growth factor is a neurotrophic factor which stimulates axonal outgrowth through the flk-1 receptor. Eur. J. Neurosci. 12, 4243–4254.

Spence, S., Poole, T., 1994. Developing blood vessels and associated extracellular matrix as substrates for neural crest migration in Japanese quail, *Coturnic coturnix japonica*. Int. J. Dev. Biol. 38, 85–98.

Sunderland, S., 1945. Blood supply of the nerves of the upper limb in man. Arch. Neurol. Psych. 53, 91.

Suri, C., McClain, J., Thurston, G., McDonald, D., Zhou, H., Oldmixon, E., Sato, T., Yancopoulos, G., 1998. Increased vascularization in mice overexpressing Angiopoietin-1. Science 282, 468–471.

Swanson, G., Lewis, J., 1982. The timetable of innervation and its control in the chick wing bud. J. Embryol. Exp. Morphol. 71, 121–137.

Swartz, M., Eberhart, J., Mastick, G.S., Krull, C.E., 2001. Sparking new frontiers: using in vivo electroporation for genetic manipulations. Dev. Biol. 233, 13–21.

Takagi, S., Tsuj, T., Amagai, T., Takamatsu, T., Fujisawa, H., 1987. Specific cell surface labels in the visual centers of *Xenopus laevis* tadpole identified using monoclonal antibodies. Dev. Biol. 122, 90–100.

Takahashi, Y., Imanaka, T., Takano, T., 1996. Spatial and temporal pattern of smooth muscle cell differentiation during development of the vascular system in the mouse embryo. Anat. Embryol. (Berl.) 194, 515–526.

Takashima, S., Kitakaze, M., Asakura, M., Asanuma, H., Sanada, S., Tashiro, F., Niwa, H., Miyazaki Ji, J., Hirota, S., Kitamura, Y., Kitsukawa, T., Fujisawa, H., Klagsbrun, M., Hori, M., 2002. Targeting of both mouse neuropilin-1 and neuropilin-2 genes severely impairs developmental yolk sac and embryonic angiogenesis. Proc. Natl. Acad. Sci. USA 99, 3657–3662.

Taniguchi, M., Yuasa, S., Fujisawa, H., Naruse, I., Saga, S., Mishina, M., Yagi, T., 1997. Disruption of semaphorinIII/D gene causes severe abnormality in peripheral nerve projection. Neuron 19, 519–530.

Taylor, G., Gianoutsos, M., Morris, S., 1994. The neurovascular territories of the skin and muscles: anatomic study and clinical implications. Plastic Reconstructive Surg. 94, 1–36.

Taylor, G., Minabe, T., 1992. The Angiosomes of the mammals and other vertebrates. Plast. Reconstr. Surg. 89, 181–215.

Teillet, M.A., Le Douarin, N.M., 1983. Consequences of neural tube and notochord excision on the development of the peripheral nervous system in the chick embryo. Dev. Biol. 98, 192–211.

Tosney, K.W., Landmesser, L.T., 1985. Development of the major pathways for neurite outgrowth in the chick hindlimb. Dev. Biol. 109, 193–214.

Upton, J., Coombs, C.J., Mulliken, J.B., Burrows, P.E., Pap, S., 1999. Vascular malformations of the upper limb: a review of 270 patients. J. Hand Surg. [Am]. 24A, 1019–1035.

Vargesson, N., Laufer, E., 2001. Smad7 misexpression during embryonic angiogenesis causes vascular dilation and malformations independently of vascular smooth muscle cell function. Dev. Biol. 240, 499–516.

Weddell, G., 1942. Axonal regeneration in cutaneous nerve plexuses. J. Anat. 77, 49–62.

Wheater, P., Burkitt, H., Stevens, A., Lowe, J., 1985. Basic Histopathology: A Color Atlas and Text. Churchill Livingstone, New York.

Whitaker, G.B., Limberg, B.J., Rosenbaum, J.S., 2001. Vascular endothelial growth factor receptor- 2 and neuropilin-1 form a receptor complex that is responsible for the differential signaling potency of vegf165 and vegf121. J. Biol. Chem. 276, 25520–25531.

Wilson, D., 1986. Development of avascularity during cartilage differentiation in the embryonic limb. Differentiation 30, 183–187.

Wilting, J., Birkenhager, R., Eichmann, A., Kurz, H., Martiny-Baron, G., Marme, D., McCarthy, J., Christ, B., Weich, H., 1996. VEGF(121) induces proliferation of vascular endothelial cells and expression of flk-1 without affecting lymphatic vessels of the chorioallantoic membrane. Dev. Biol. 176, 76–85.

Wilting, J., Eichmann, A., Christ, B., 1997. Expression of the avian VEGF receptor homologues Quek1 and Quek2 in blood-vascular and lymphatic endothelial and non-endothelial cells during quail embryonic development. Cell Tissue Res. 288, 207–22.

Wright, D.E., White, F.A., Gerfen, R.W., Silossantiago, I., Snider, W.D., 1995. The guidance molecule semaphorin-III is expressed in regions of spinal-cord and periphery avoided by growing sensory axons. J. Comp. Neurol. 361, 321–333.

Yamada, Y., Takakura, N., Yasue, H., Ogawa, H., Fujisawa, H., Suda, T., 2001. Exogenous clustered neuropilin 1 enhances vasculogenesis and angiogenesis. Blood 97, 1671–1678.

Yang, Y., Drossopoulou, G., Chuang, P.T., Duprez, D., Marti, E., Bumcrot, D., Vargesson, N., Clarke, J., Niswander, L., McMahon, A., Tickle, C., 1997. Relationship between dose, distance and time in Sonic Hedgehog-mediated regulation of anteroposterior polarity in the chick limb. Development 124, 4393–4404.

Yin, M., Pacifici, M., 2001. Vascular regression is required for mesenchymal condensation and chondrogenesis in the developing limb. Dev. Dyn. 222, 522–533.